Advanced Functional Nanomaterials for Theranostics

*Haoyuan Huang and Jonathan F. Lovell**

Nanoscale materials have been explored extensively as agents for therapeutic and diagnostic (i.e., theranostic) applications. Research efforts have shifted from exploring new materials in vitro to designing materials that function in more relevant animal disease models, thereby increasing potential for clinical translation. Current interests include non-invasive imaging of diseases, biomarkers, and targeted delivery of therapeutic drugs. Here, some general design considerations of advanced theranostic materials and challenges of their use, from both diagnostic and therapeutic perspectives, are discussed. Common classes of nanoscale biomaterials, including magnetic nanoparticles, quantum dots, upconversion nanoparticles, mesoporous silica nanoparticles, carbon-based nanoparticles, and organic dye-based nanoparticles, have demonstrated potential for both diagnosis and therapy. Variations such as size control and surface modifications can modulate biocompatibility and interactions with target tissues. The need for improved disease detection and enhanced chemotherapeutic treatments, together with realistic considerations for clinically translatable nanomaterials, will be key driving factors for theranostic agent research in the near future.

1. Introduction

Medical interests related to nanotechnology have expanded during recent decades. Several classes of nanomedicines have been translated at least to early phase clinical testing.[1] Common biomedical functional nanocarriers are shown in **Figure 1**, including liposomes, polymeric micelles, dendrimers and inorganic nanocarriers.[2] With incorporation of imaging and therapeutic agents, biocompatible nanoscale carriers can offer improved biodistribution and reduced toxicity. In some cases, the carrier itself comprises imaging and therapeutic properties.[3] Unlike traditional small molecule agents, theranostic functional nanomaterials hold potential to enhance the delivery of pharmacological agents and guide the nanoparticles following administration, in order to maximize therapeutic efficiency and minimize off-target toxicity.[4] By combining drugs and imaging contrast agents within a single specific modified platform, these theranostic systems enable the possibility of monitoring of passive and active targeting, triggered release and other therapeutic functions.[5,6]

H. Huang, Prof. J. F. Lovell
Department of Biomedical Engineering
University at Buffalo
State University of New York
Buffalo, New York 14260, United States
E-mail: jflovell@buffalo.edu

DOI: 10.1002/adfm.201603524

Engineering multifunctional theranostic nanoparticles presents numerous challenges.[7] These include material requirements for providing sufficient imaging or therapeutic loading; toxicity of intrinsic components; storage and in vivo stability; production complexity; batch-to-batch variation; manufacturing costs; and regulatory hurdles have created challenges which impeded clinical development.[8,9] Furthermore, design of theranostic materials generally requires development on a case-by-case basis. For example, imaging contrast agents could ideally operate with fast target tissue binding and fast clearance from blood, whereas for drug delivery, longer circulation is required for sufficient uptake in target tissues. Likewise, the physical parameters of loaded cargos (e.g., hydrophobic drugs, polyionic nucleic acids, small hydrophilic imaging contrast agents) vary considerably so that different material strategies are required for effective loading. Thus, it is difficult to generalize any single type of material for all theranostic applications. In the following sections, we discuss diagnostic imaging technologies, nanocarriers, toxicity, pharmacokinetics, as well as introducing details of several common theranostic nanoparticles, classified by their compositions and properties.

2. Imaging Modalities

Molecular imaging allows for characterization and measurement of biological processes in intact organisms at cellular or subcellular levels.[10] By using specific molecular probes or contrast agents, imaging can, in some cases, monitor and describe disease progress in a clinically useful manner. Current imaging modalities include MRI (magnetic resonance imaging), CT (X-ray computed tomography), US (ultrasound), optical imaging (fluorescent and luminescent imaging) and PAT (photoacoustic tomography), positron emission tomography (PET), and single photon emission computed tomography (SPECT) (**Figure 2**).[5]

Quantitative measures of molecular imaging contrast agents are desired for establishing automated algorithms and guidelines for diagnostic non-invasive medical imaging. However, since each imaging technique has its own advantages and limitations, the proper combinations of different imaging techniques can potentially maximize efficiencies and assist in next generation diagnostic approaches.[11,12] It is desirable to develop a single contrast agent suitable for multiple imaging modalities.

2.1. Optical Imaging

Optical imaging is a common modality in preclinical research of theranostic nanomaterials. This technique generally detects emitted photons from probes after they absorb light. Compared to other imaging modalities, optical imaging is relatively inexpensive and avoids harm associated with ionizing radiation. However, the drawbacks of optical imaging are significant. Contrast agents are often excited by visible or ultraviolet light (UV), which cannot penetrate in deep tissues, and the emitted fluorescence signals are sensitive to noise due to the scattering of photons from surrounding tissues[13] or light-absorbing proteins, heme within red blood cells, and even water.[14] In this context, fluorophores in the near-infrared (NIR; 650–1000 nm) show promise by reducing autofluorescence and photon scattering to allow deeper tissue penetration, making optical imaging more suitable for in vivo applications. Nevertheless, even NIR imaging is limited to relatively shallow depths in tissues, which are suitable for rodent imaging. Although NIR-active nanomaterials have been shown to be capable of preclinical tumor imaging, this paradigm has had some but limited translation to humans. Possibly, this is because large tumors or other conditions in humans are generally satisfactorily detected with MR or CT. Optical imaging is also not an ideal modality to detect metastatic dissemination in humans, due to limited scan size. However, it should be noted that several clinical stage companies are developing NIR imaging systems, largely in the context of image-guided surgery and nanomaterials have potential more sophisticated approaches compared to current small molecule NIR dyes such as indocyanine green.[15–17]

2.2. Magnetic Resonance Imaging

MRI is based on the behavior of water hydrogen nuclei under an applied magnetic field. By applying radiofrequency pulses and magnetic field gradients, the relaxation process of the nuclei return to the original aligned states and this process is recorded and converted into images.[18] MR can image soft tissues in humans with whole body depth and high resolution without the need for contrast agents. However, MR contrast agents can further enhance MRI signals in two ways: reducing T1 (referred to as longitudinal relaxation time; spin-lattice relaxation time) or T2 (referred to as transverse relaxation time; spin-spin relaxation time) relaxation time of water protons. Thus MR contrast agents are generally divided in two classes: T1 contrast agents, which are typically paramagnetic complexes (like Gd^{3+} complexes); and T2 contrast agents, which are typically iron oxide based nanoparticles.[19] Such inorganic nanoparticles possess large surface area for enhancing contrast effects.[20] There are a number of MR contrast agents undergoing clinical trials and some of them have been approved for clinical applications.[21–23] Compared to in vivo fluorescence imaging, MR can provide better spatial resolution without depth limitations. However, MR has drawbacks such as a relatively high cost of use and poor sensitivity to contrast agents, given the abundance of water in the human body. To achieve better imaging quality, a large administered quantity of contrast agent is required. This large dose is challenging to administer without toxicity concerns.

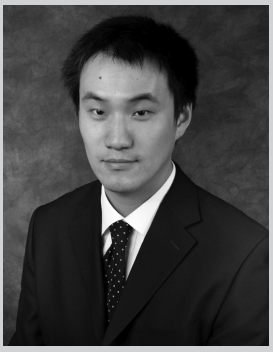

Haoyuan Huang obtained his B.S. degree from the department of Polymer Science and Engineering at Zhejiang University in China. He started in 2012 as an inaugural graduate student member of the group of Dr. Jonathan Lovell at University at Buffalo, State University of New York. Since completing an M.S. degree in Chemical and Biological Engineering, he has continued onto Ph.D. studies in Biomedical Engineering. His current research involves synthesis and application of theranostic porphyrin-related polymers.

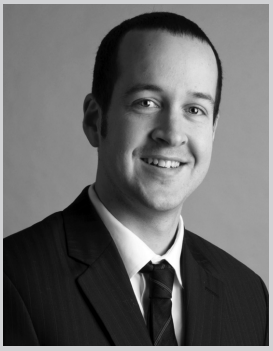

Jonathan Lovell is an Assistant Professor in the Biomedical Engineering Department at University at Buffalo. He received a Ph.D. from the Institute for Biomaterials and Biomedical Engineering at University of Toronto, working in the lab of Dr. Gang Zheng. Previously, he completed an M.S. degree in Biochemistry at McMaster University and his undergraduate degree at the University of Waterloo in Systems Design Engineering. His research interests involve developing safe, novel, and translatable nanoplatforms to address unmet medical needs.

2.3. Positron Emission Tomography

PET contrast agents are positron emitting radionuclide-containing materials. These materials decay by releasing a positively charged subatomic particle; a positron. The positron will travel a short distance within the surrounding tissues before it annihilates with an electron. The annihilation will then release two opposite-direction γ-rays, which will be recorded by surrounding detectors and transferred to computed images.[24] The contrast agents are usually radio-isotopes, like ^{11}C, ^{13}N, ^{68}Gd, ^{64}Cu, ^{76}Br, ^{124}I and ^{18}F. The travel distance of the positrons is different between each contrast agent, and usually higher energy positrons will travel longer distance before annihilation and cause higher loss of spatial resolution. Radioactive PET contrast agents demonstrate indistinguishable chemical properties before and after radioactive decay, so that radioactive-independent physiological properties of the agents remain stable. PET is a quantitative technique and the amounts

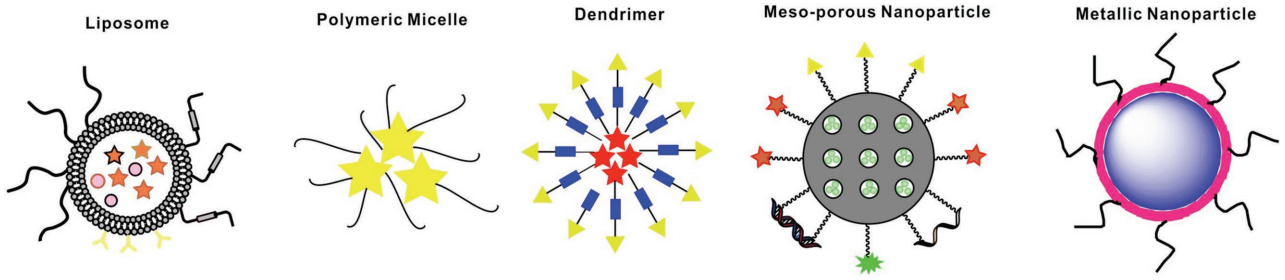

Figure 1. Schematic representation of selected nanocarriers. Stars, circles, and triangles represent various possible and hypothetical modifications such as payloads, cargo, imaging agents, and targeting moieties. Reproduced with permission.[2] Copyright 2011, American Chemical Society.

of contrast agent signal in various observed volumes can be calculated readily. Currently, the combination of PET and MRI imaging instrumentation has been developed for clinical imaging with signal co-registration. With increasing interest in dual function imaging probes, the PET/MRI combination is one of the most clinically relevant.[25,26]

2.4. Ultrasound

Ultrasound is a commonly used clinical diagnostic imaging modality. Compared to other techniques, the cost is low, operation is simple, detection is in real time and there are no safety concerns. By emitting high frequency sound waves from the transducer against the skin, an US image is generated from the reflection of sound wave from internal objects and organs.[27] Ultrasound contrast agents focus on providing higher resonance frequencies in areas under observation.[28] Nearly 20 contrast agents have been used in the clinic.[29] However, even with these US contrast agents, the resolution is relatively low as there is a fundamental trade-off between depth and resolution.

2.5. Photoacoustic Tomography

As early as 1880, Alexander Graham Bell reported the phenomena of light being used to generate sound waves. In the past couple of decades, this technique has been extensively explored for biomedical applications.[30] Photoacoustic tomography (PAT) images are generated by light-induced pressure waves. Briefly, a target volume is irradiated with a short-pulse laser beam, and a portion of that light will be absorbed by endogenous or exogenous contrast agents and transferred to heat and converted to pressure via thermoelastic expansion. This pressure rise propagates as an acoustic wave detected by conventional

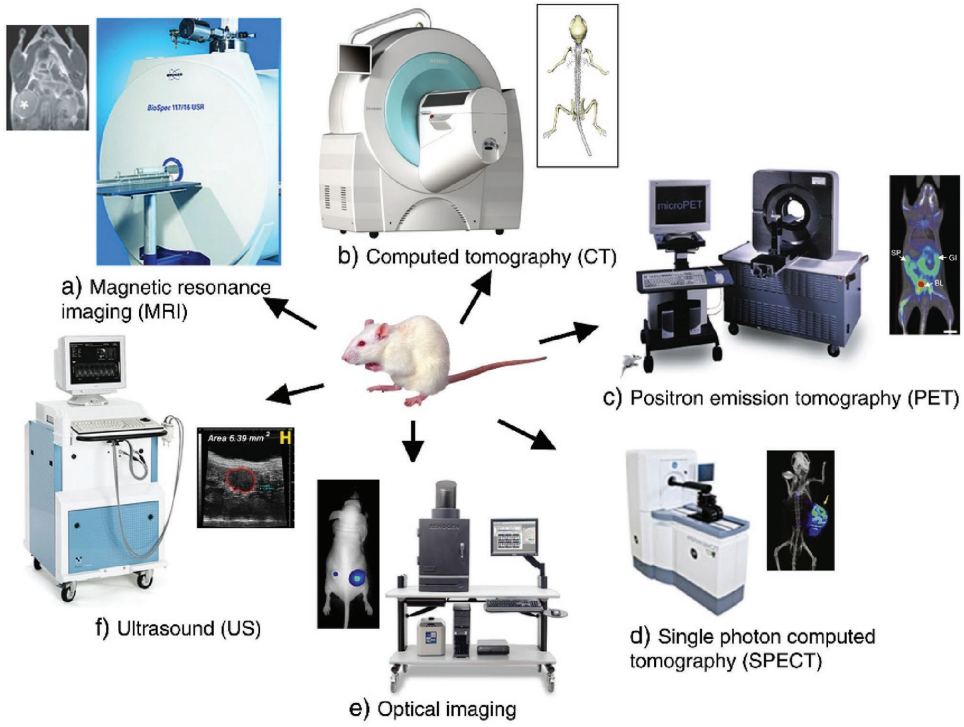

Figure 2. Molecular imaging instrumentation and images for common diagnostic modalities. Reproduced with permission.[5] Copyright 2010, Elsevier.

ultrasonic transducers.[31] PAT can reduce optical tissue scattering, generate multiscale high resolution images, provide high signal-noise ratio due to the small background, there is no leakage of excitation photons into detectors and speckle-free images are produced.[32] Contrast-enhanced PAT can operate significantly deeper than any other optical imaging techniques and there have been reports of PAT contrast-enhanced imaging through over 10 cm of chicken breast tissue and 5 cm through a human arm.[33] As an emerging diagnostic technique, PAT has been demonstrated successfully in a range of preclinical experiments, and further clinical studies are ongoing.

3. Therapeutic Approaches

The other key application of theranostic nanoparticles is therapy. Nanoparticles have frequently been applied for cancer therapy. Some conventional therapeutic methods include chemotherapy, photothermal therapy and photodynamic therapy. Chemotherapy employs toxic therapeutic drugs, which are able to interfere with the molecular activities of cancer cells. Several drugs are used in cancer treatment, like doxorubicin (DOX), methotrexate (MTX) and cabazitaxel (CTX).[34,35] However, chemotherapy often requires several doses, which may cause significant side effects. Another treatment method is photothermal therapy. Light-absorbing agents can transfer light energy to heat, leading to tumor ablation. The ideal photothermal agents should have large absorption cross section in any of the biological windows (the first window being 700–980 nm and the second one is 1000–1400 nm), low toxicity, and good biocompatibility.[35] Inorganic materials such as gold nanoparticles,[36,37] nanographene[38] and other inorganic nanoparticles, as well as NIR absorbing organic materials[39,40] have achieved preclinical success in photothermal therapy.

Photodynamic therapy uses singlet oxygen generated from photosensitizers under light exposure to eliminate cancer cells. There are a wide range of photosensitizer molecules, especially porphyrins and related molecules that have widely been used for cancer treatments, some progressing to the clinic. With laser irradiation at an appropriate wavelength, photosensitizers will generate cytotoxic oxygen species and consequently kill cancer cells. To enhance treatment efficiency and reduce side effects, the development of tumor-targeting delivery vesicles is an area of interest.

4. Nanocarriers

Commonly used nanocarriers include organic carriers (e.g., liposomes, micelles, dendrimers) and inorganic carriers (e.g., hollow/porous nanostructures, metallic nanocrystals and carbon nanomaterials). These nanoscale materials can be loaded with both imaging and therapeutic payloads by physical encapsulation or chemical conjugation. The carriers that physically encapsulate internal functional payloads have some type of porous structure to enable loading, but not all payloads need to be entrapped in the carriers during their formation. Various intermolecular interactions can be used during the loading process, such as ionic forces, hydrogen bonds and covalent bonds. The main functions for the carrier is to deliver the diagnostic and therapeutic containments as stealthily and selectively to the target area while minimize adverse side effects induced by premature drug release.

4.1. Liposomes

Liposomes have been studied for more than half a century and numerous formulations have entered clinical applications.[41–43] Liposomes demonstrate favorable biocompatibility with high and stable loading efficiency, and are generally one of the most clinically translatable nanocarriers. In addition, there are various methods to modulate liposomes to achieve more selective targeting and more effective drug delivery.[44–46] Furthermore, some modifications allow liposomes for environment-triggered drug releasing.[47,48] However, liposomes also demonstrate disadvantages that could limit their clinical applications. Compared to small molecule drugs, liposomes add a substantial layer of complexity, complicating regulatory issues. As a general solubilizer of cargo, liposomes must compete with biocompatible surfactants like Tween and Cremophor, which are probably simpler to create formulations with. Like other carriers, premature release of cargo caused by the instability of liposomes is detrimental, whereas if the carriers are overly stable, drug release and bioavailability at the target site may be non-ideal.

Porphyrin molecules have been directly conjugated to lipids in order to assemble modified liposomes termed porphysomes.[49] Unlike the traditional encapsulation, porphyrin molecules became a component of the nanoscale carrier itself. Porphysomes directly possess intrinsic theranostic functions. Moreover, by loading with other drugs, this new kind porphyrin-containing liposomes can achieve multiple types of theranostic efficiency.

4.2. Polymeric Micelles

Formed with amphipathic units that are self-assembled in water, micelles can encapsulate a wide range of diagnostic or therapeutic payloads through intermolecular interactions or direct conjugation. Amphiphilic block copolymers can entrap hydrophobic molecules in their core to form micelles that solubilize the cargo.[50] Due to the influence of the cargo on the micelle formation process, cargo is encapsulated into micelles during the self-assembly process.[51] Micelles can solubilize even extremely hydrophobic materials and in some cases, the excess surfactant can be stripped away to bypass toxicity compared to the simpler approach of dissolving the cargo directly in surfactants.[52,53] Furthermore, by choosing the proper micelle unimer, the release rate of cargo can be controlled. These responsive micelles enable triggered degradations under certain physiological conditions, such as pH, light, singlet oxygen molecules.

4.3. Dendrimers

Dendrimers are polymeric hyper-branched nanostructures that, compared to other nanocarriers are chemically well-defined.

Monomers combine to form spherical nanostructures, with a core suitable for loading and defined nodes that theranostic agents can be chemically grafted onto.[54] The synthesis process can be precisely regulated, thus determining optimal compositions for biomedical applications.[55] The well-defined structures and high cargo carrying capacity makes dendrimers promising nanocarriers for theranostic applications including gene delivery, molecular imaging and tumor therapy.[56] However, long-term carrier clearance and biocompatibility need to be addressed for advancing clinical applications.

4.4. Hollow or Porous Nanocarriers

Several inorganic nanocarriers with hollow or porous structures have been developed. Examples include mesoporous silica nanoparticles, hollow gold nanoparticles, and calcium phosphate nanoparticles. Carbon nanotubes and graphene have also been developed as mesoporous materials. The surface of carbon nanotubes and graphene can be modified with other organic groups such as carboxylic acids or alcohols so they can be covalently linked with theranostic cargoes. Alternatively, drugs can adsorb through molecular interactions such as π–π stacking.[57–60] These modifications can improve the solubility, biocompatibility for these hollow materials for biomedical applications.

4.5. Metallic Nanoparticles

There are several different kinds of metallic nanoparticles used in theranostics, such as magnetic nanoparticles, gold nanoparticles, upconversion nanoparticles, and inorganic quantum dots. These materials have been widely used as contrast agents for various imaging modalities. They have also been combined with therapeutic agents to achieve image-guided treatments and to predict therapeutic responses.[61] Moreover, several of these materials are possess photothermal efficacy in order to convert light to heat. These materials are discussed further in Section 8.

5. Toxicity

Poorly defined toxicity is increasingly being recognized as a main barrier to clinical translation of new nanomaterials. The physicochemical properties of nanomaterials affect toxicity after administration. Physical parameters such as size, agglomeration state, shape, surface charges, critical structure as well as chemical properties like surface modification, and chemical compositions influence pharmacokinetic and toxicity properties.[62,63] Nanoparticle toxicity in organs can occur with inflammation and generation of reactive oxygen species (ROS).[64] High levels of ROS will cause damage and disruption to several cellular process, which can be generated from the innate immune response to nanoparticles or from specific nanoparticles that autocatalyze ROS formations.[65] Even though in vitro tests can identify potential nanoparticle toxicity, the in vivo mechanisms are more complex. After administration, nanoparticles will interact with inherent biological proteins and will distribute to different critical organs, where it can be difficult to predict how they will influence organ function and for how long they will persist there.

6. Pharmacokinetics and Pharmacodynamics

Therapeutic efficiency is dependent on the therapeutic payloads reaching target tissues and becoming bioavailable. If the therapeutic agent dislodges from the carrier immediately upon administration in the body, the role of the nanocarrier is little more than a solubilizing agent. If the nanocarrier modulates the behavior of the payload in the body, the pharmacokinetics (PK) and pharmacodynamics (PD) become key quantifiable properties of this process. The therapeutic agents will act for treatments after they reaching the target area and response to certain stimulations. There are two common excretion routes to remove administrated materials: through urinal excretion or via liver metabolic pathways. In general, only a small fraction of nanomaterials will reach target tissues, with non-target organs such as the liver and spleen receiving the bulk.[66] Some promising theranostic agents have toxicity concerns, like QDs, which may potentially induce heavy metal poisoning. However, all materials require detailed toxicological characterization prior to any clinical studies.

PK quantifies the fate and location of administrated agents in living organisms. PD examines the physiological properties of the drug in vivo, such as encapsulation status.[67] Chemical modifications of nanocarriers modulates these properties. As an example, following intravenous administration, protein opsonization will mark numerous bare carriers, for macrophage uptake. To overcome this, a common strategy is to coat the materials with polyethylene glycol (PEG). Surface modification with PEG can create stealth nanoparticles with substantially prolonged blood circulation.[68] The size and morphology of nanoparticles impacts PK; for example materials will be excreted rapidly by the renal system when their sizes are smaller than 5.5 nm or their molecular weights are lower than 60 kDa.[69,70] It is therefore important to scrutinize the design and therapeutic efficiency of theranostic agents with regard to PK and PD. This information is also essential from a regulatory point of view prior to human trials.

7. Design of Nanoparticles

Proper design of nanoparticles is critical. Engineered nanoparticles are typically comprised with biomedical payloads, nanocarriers and surface modifiers, as shown in **Figure 3**.[67] The payloads could include imaging agents, therapeutic drugs, and even other nanoparticles such as quantum dots, upconversion nanoparticles, or magnetic nanoparticles. Carriers can alter the solubility or PK/PD of theranostic agents. Surface ligands can interact with the physiological environment to achieve active targeting. Ideally, ligand coated nanoparticles concentrate to target site via the recognition of ligand receptors overexpressed on the surface of target cells. Numerous targeting ligands have been reported.[71] Surface modification also modulates blood circulation times.

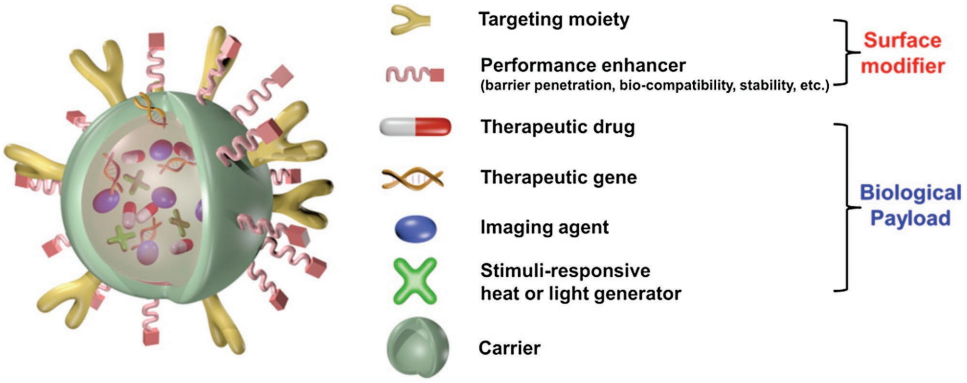

Figure 3. A prototypical multifunctional nanoparticle. Reproduced with permission.[67] Copyright 2015, American Chemical Society.

8. Theranostic Nanomaterials

8.1. Magnetic Nanomaterials

Magnetic nanomaterials have been widely applied for in vitro and in vivo theranostic studies. Magnetic nanomaterials can operate as an MRI contrast agent and for anti-cancer treatment. Magnetic nanoparticles can be precisely tailored with variable size, composition, morphology, and surface modifications. These controllable physical and chemical properties can enhance magnetic features and in vivo behavior.[72,73] Colloidal iron oxide nanoparticles, which are usually comprised of nanocrystalline magnetite (Fe_3O_4) or maghemite (γ-Fe_2O_3), are the most prominent. The main methods for synthesizing magnetic nanoparticles, such as Fe_3O_4 nanoparticles, include physical methods, wet chemical preparation, and an emerging method, metal-doped iron oxides.[74] The physical properties of magnetic nanoparticles can determine their magnetic properties; superparamagnetism occurs when the diameter is smaller than 50 nm and soft ferri- or ferromagnetism occurs when the particles are smaller than 100 nm.[75,76]

Magnetic clusters are prone to aggregation. To bypass this, they can be stabilized through carrier interactions or surface modifications, as reflected in **Figure 4**.[72] The outer coating of the magnetic nanoparticles not only influences the overall size, but also the pharmacokinetics, biodistribution and toxicity profile in vivo. Surface modification can bring different surface charges, thermodynamic properties and environmental sensitivities. PEGylated magnetic nanoparticles enable prolonged blood circulation time for long-term blood pool MRI and this size is suitable for the enhanced permeability and retention (EPR) effect to take advantage of irregular tumor vasculature.

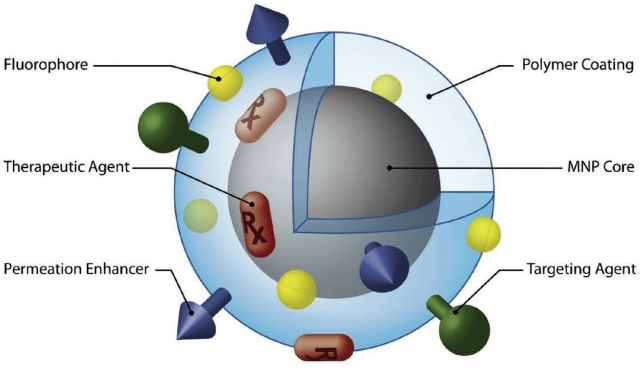

Figure 4. Schematic figure of multifunctional magnetic nanoparticles with surface coating. Reproduced with permission.[72] Copyright 2008, Elsevier.

8.1.1. Magnetic Nanoparticles as MRI Contrast Agents

MRI is one of the most widely used diagnostic imaging techniques with the capability of providing high resolution anatomical images. Magnetic nanoparticles are used to enhance MR signal intensities of areas of interest under both T1 and T2 modalities. Although long-term commercial viability remains to be determined, several magnetic nanomaterials have been clinically approved or are undergoing clinical trials, such as Ferumoxsil.[74] Magnetic nanoparticles can be combined with therapeutic drugs for monitoring the drug delivery or treatment efficiency.

During recent years, research efforts have focused on incorporating additional imaging techniques with MRI to gain additional information and overcome the inherent limitations of single modality imaging. As a versatile platform, magnetic nanoparticles offer the ability to generate contrast in several different imaging techniques. For example, MR-optical imaging, MR-PET imaging and MR-photoacoustic imaging have been explored.[77–79]

One of the most well-known MR contrast agents is superparamagnetic iron oxide nanoparticles (SPIONs). This type of magnetic nanomaterial demonstrates prolonged T2 and T2* effects.[80] The inner magnetic cores for SPIONs are magnetite (Fe_3O_4), maghemite (γ-Fe_2O_3) and hematite (α-Fe_2O_3).[81] The physical and biomedical properties, such as improving stability, blood circulation time and selectivity, can be adjusted by the selection of surface properties. Reported coating materials include PEG,[82,83] PAA,[84] peptides or proteins,[85,86] aptamers[87] and zwitterionic compounds.[88] Radionuclides have been incorporated with SPIONs for multimodal imaging. ^{64}Cu was functionalized to SPIONs through diphosphonate groups.[89] 3 h post injection of their samples in the footpads, the contrast agents concentrated to the lymph nodes and enabled clear PET and MRI imaging. In 2014, Chakravarty et al. demonstrated

the feasibility of PEGylated ^{69}Ge-labled SPION for PET/MRI imaging (**Figure 5**a).[90] Compared to free ^{69}Ge, the labeled PEGylated nanoparticles overcame fast renal clearance and demonstrated long-term stability, and both PET and MRI showed clear lymph node imaging (Figure 5b and 5c).[90] It has been shown that Gadolinium can be chelated with SPIONs for T1- and T2-weighted contrast MRI and this imaged U87-MG tumors in vivo.[91] SPIONs can also serve as a drug delivery platform for MRI guided therapy.[92–96] Interestingly, besides T2-weighted imaging, some Fe_3O_4 based SPIONs were developed with T1-weighted contrast.[97–100] These findings demonstrate the possibility for using SPIONs as potential T1-weighted MRI, which is generally simpler for image interpretation.

Besides iron-based magnetic nanoparticles, ^{19}F, manganese and gadolinium agents have been used for MRI contrast. The body contains little fluorine background in soft tissues, and special MR pulse sequences are used to directly detect ^{19}F. However, to achieve satisfactory image quality, a large amount of administered ^{19}F is required. To address this, fluorine-rich perfluorocarbons have been explored as ^{19}F MR contrast agents.[101] Several functional probes have been demonstrated at the molecular or cellular levels.[102–107] Moreover, a variety of fluorocarbon nanoparticles have been applied for in vivo applications, such as for detection of vessel occlusions in cerebral photothrombosis,[108] monitoring arthritic inflammation therapy,[109] and quantifying muscle oxygenation.[110]

Gadolinium and manganese are paramagnetic metals which can produce T1-weighted MRI contrast. Due to toxicity of the free metal, Gd-based MRI contrast agents are commonly chelated with acyclic or macrocyclic chelating ligands (**Figure 6**).[111–113] Gd can be incorporated into other materials like silica nanoparticles,[114,115] liposomes,[116] hydrogels,[117] dendrimers[118,119] or can be directly linked with biomolecules.[120–123]

Manganese (Mn)-based nanomaterials are active in T1-weighted MRI. Mn plays vital endogenous roles in the body, such as in mitochondrial function, therefore it represents an endogenous metal, unlike Gd.[124] Mn-based MRI contrast agent have been used in studying retina and brain,[125–127] neuronal activity,[128] cancers,[129,130] and other animal disease models such as Alzheimer's,[131] atherosclerotic Lesions,[132] mesial temporal lobe epilepsy,[133] and schizophrenia.[134] By using the ^{52}Mn radioisotope, it could be possible to use Mn for both PET and MRI, and this was exemplified in a stem cell tracking study with stem cells overexpressing a divalent metal transporter.[135]

8.1.2. Magnetic Materials for Therapy

When subjected to alternating magnetic fields, magnetic materials can be heated to induce hyperthermia.[136] These effects are size-dependent.[137] Numerous studies have demonstrated

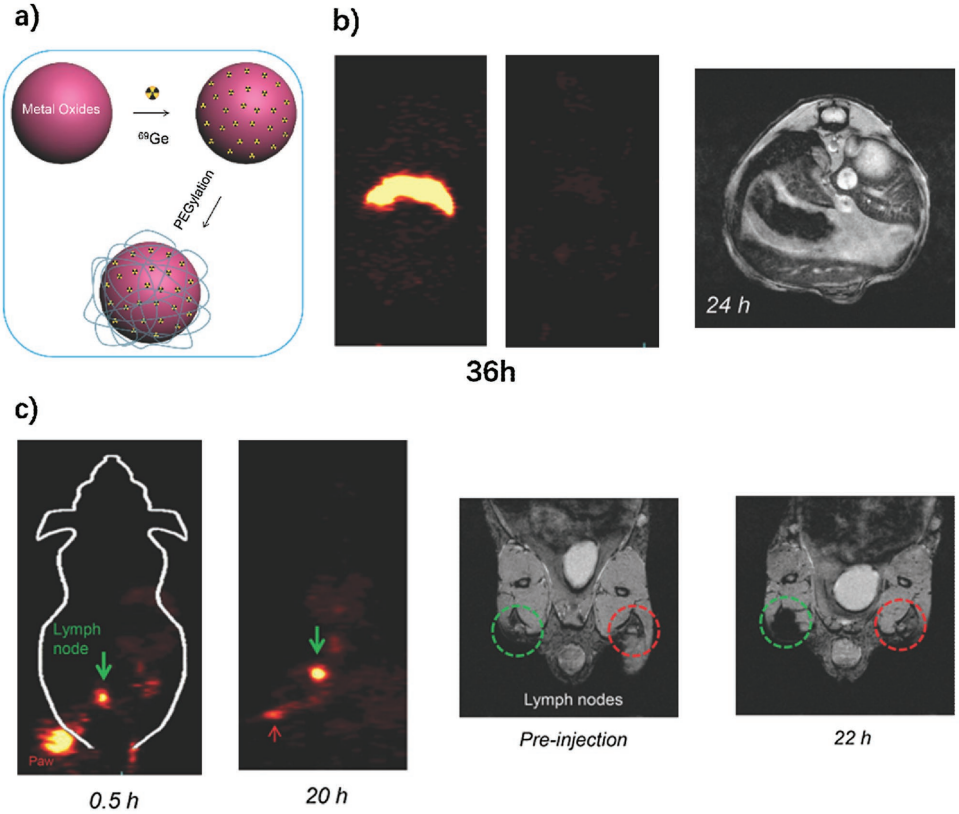

Figure 5. ^{69}Ge-labled SPION for PET/MRI. a) Schematic figure of ^{69}Ge labeling SPIONs; b) biodistribution monitoring post i.v. injection through PET and MRI. Contrast agents demonstrated long-term signals 36 h post injection with PET imaging and 24 h with MRI; c) Long-term lymph node mapping with PET and MRI. The green circle areas for MRI images are contrast agents injected position and the red areas are control areas. Reproduced with permission.[90] Copyright 2014, Wiley.

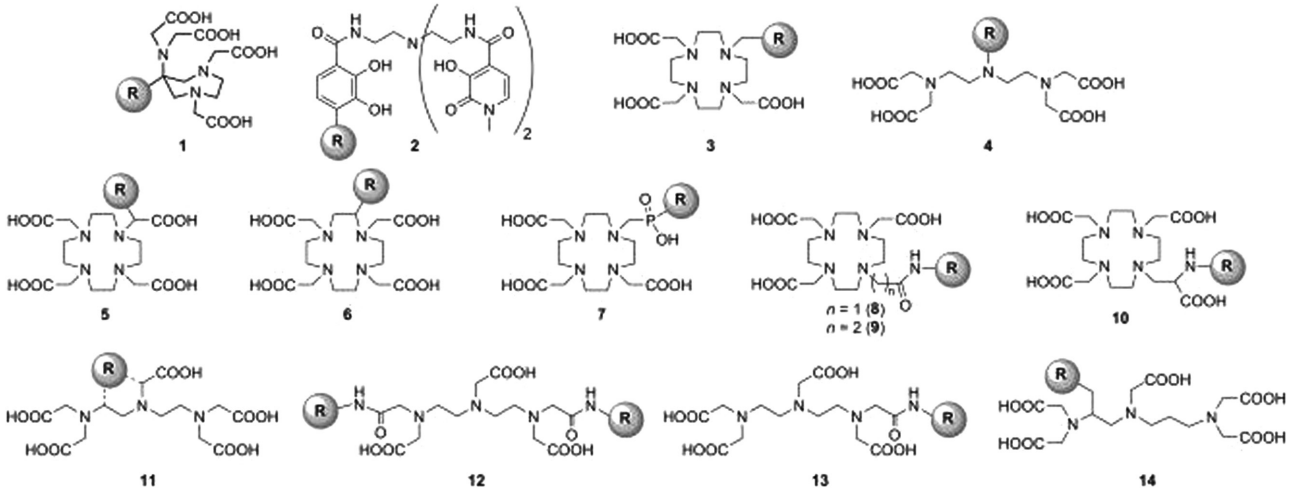

Figure 6. Structures of some common Gd chelators. Reproduced with permission.[111] Copyright 2012, Wiley.

magnetic hyperthermia anti-cancer functions in vitro.[138–141] These studies are also increasingly being demonstrated in in vivo models.[142–144] Corato et al. combined photothermal and photodynamic therapy together with iron oxide nanoparticles in Foscan modified liposomes.[145]

Besides hyperthermia, magnetic nanoparticles have been used for photothermal applications.[146,147] Espinosa et al. synthesized magnetite iron oxide nanocubes as a dual functional agent for magnetic hyperthermia and photothermal therapy.[148] The heating capacity of the magnetophotothermal nanocubes reached 4850 W g^{-1}, nearly 5 times greater than efficiencies reported for iron oxide magnetic nanoparticles. In vivo study, the dual-modality treatment induced superior tumor ablation.

Hyperthermia of magnetic materials can be also used for stimuli triggered release. Magnetic mesoporous silica nanoparticles were developed that were capped with heat-sensitive DNA molecules, so that heat generated by magnetic components triggered the capped DNA molecules to release encapsulated drugs.[149] Yin et al. designed a magnetic silica nanoparticle complex for delivering and activating heat-inducible adipose-derived mesenchymal stem cells with expression of TNF-related apoptosis-inducing ligand (TRAIL).[150] Magnetic hyperthermia helped control selective expression of TRAIL for gene therapy in ovarian cancer in in vitro and in vivo studies.

8.1.3. Magnetic Theranostic Nanoparticles

Because MRI is a broadly used clinical diagnostic technique, magnetic nanoparticles hold potential as theranostic agents. By combining magnetic nanoparticles with other functional molecules, MRI diagnostic images can be enhanced to visualize diseased tissues and monitor the process of treatment.[151,152] Several cancer treatment drugs have been combined with magnetic nanoparticles for MRI-guided chemotherapy, such as paclitaxel (PTX)[153,154] and DOX,[155–157] Lee et al. used urokinase plasminogen activator receptor (uPAR)-targeted magnetic iron oxide nanoparticles as carriers to delivery gemcitabine to uPAR-expressing tumors and stromal cells.[158] The system showed an enhanced MRI signal in orthotopic human pancreatic cancer xenografts in nude mice, which could help detect the tumor position and determine the drug resistance. Song et al. developed Co_9Se_8 nanoparticles for PAT and MRI tumor diagnosis and monitoring.[159] This nanoparticulate system enabled chemotherapy and photothermal therapy together by loading with DOX, which enhanced treatment efficiency.

Other theranostic approaches use magnetic nanoparticles for both imaging therapeutic functions since the nanoparticles themselves can be used as hyperthermia agents. By applying an external magnetic field, magnetic nanoparticles can generate heat to increase the temperature of targeted tissue and ablate the tumor. Magnetic nanoparticles can also help diagnose the tumor location inside body and monitor the treatment efficiency.[160] Hayashi et al. used superparamagnetic nanoparticle clusters for cancer therapy.[161] These folic acid and PEG co-coated nanoparticles showed strong T2-weighted MRI images in the tumor, and by applying an external magnetic field, the temperature was raised about 6 °C higher than the surrounding tissue, which sufficiently inhibited tumor growth for 12 weeks. Some magnetic nanoparticles have been combined with carbon dots, which can generate heat after exposure with NIR light. Yu et al. developed Fe_5C_2 nanoparticles for MRI-PAT guided photothermal therapy.[162] The carbon shell offers the possibility of PAT imaging and photothermal therapy after irradiation with NIR laser. The magnetic inner core demonstrated MRI monitoring ability, which helps diagnostic the tumor in nude mice and monitored the treatment efficiency for as long as 45 days.

8.2. Quantum Dots

Colloidal semiconductor quantum dots (QDs) are nanocrystals with diameters typically ranging from 2–10 nm. The emission wavelength of QDs can be tuned from visible to NIR. QDs possess several unique optical properties such as high fluorescent quantum yield, size-tunable emission and high photostability.[163,164] They demonstrate a wide range of excitation wavelengths incorporated with narrow and symmetric

emission spectra. High photostability makes them suitable for long-term dynamic in vivo monitoring applications.[165,166] QDs were introduced for mainstream biomedical applications nearly two decades ago.[167,168] They remain as powerful tools for a various application including disease detection and single particle tracking.[169]

8.2.1. Biomedical Applications of Quantum Dots

QDs are useful fluorescent agents and they have well-developed surface chemistry and thus they have been used in a wide range of biomedical applications.[170] QDs have been applied for cell tracking,[171] fluorescence life-time imaging,[172] NIR imaging,[173–175] monitoring molecular functions within living cells,[176] cancer specific imaging,[177–179] gene delivery,[180,181] drug delivery[182] and photodynamic therapy.[183] NIR-active QDs are useful for in vivo imaging applications due to superior light penetration and lower scattering compared to shorter wavelengths. Erogbobgo et al. synthesized silicon QDs through acidic etching.[177] Compared to metallic QDs, silicon QDs like those shown in **Figure 7** pose lower intrinsic toxicity risks. In that study, PEGylated micelles encapsulating Si-QDs were conjugated with RGD peptides targeting $\alpha_v\beta_3$ and the nanoparticles demonstrated good imaging of tumors. Non-targeted Si-QDs could be used with NIR imaging for sentinel lymph node mapping.

In 2013, Shibu et al. raised a nanoparticle termed as photouncaging bimodal nanoparticles (PUNPs) which is comprised of photouncaging surface ligands, CdSe/ZnS QDs and super paramagnetic iron oxide.[184] By further conjugation with peptide hormones, PUNPs showed low toxicity to cells in vitro, and offers the potential to trace nanoparticles with both NIR and MRI modalities. The nanoparticles can be fully removed through renal system 48 h post injection. Recently, Han et al. conjugated mAbs to QDs which is coated with norbornene-displaying polyimidazole ligands.[185] After injection, their QDs possessed single cell labelling in bone marrow, especially the rare populations of hematopoietic stem and progenitor cells.

QDs can be doped with metallic elements for dual-modality imaging. Magnetic metal ions[186] and radioisotopes[178] were doped into QDs to confer MRI and PET imaging capabilities, respectively. Zhao et al. used cell-derived microvesicles (MVs) to entrap Mn-contained QDs for dual-modality real time tracking in vivo (**Figure 8**).[187] Ag_2Se@Mn QDs demonstrated 13% NIR fluorescence quantum yield with a longitudinal relaxivity almost four times higher than a Gd-DPTA standard. With the assistance electroporation, the 1.8 nm QDs were efficiently loaded into MVs and demonstrated strong NIR and MRI signals. QDs labelled MVs not only allowed long-term non-invasive whole body dual-modality real-time tracking, but also offer dynamic quantitative biodistribution analysis.

Yong et al. demonstrated that WS_2 QDs were not only suitable for X-ray computed tomography (CT) and photoacoustic tomography (PAT), but also worked as agents for photothermal therapy and radiotherapy.[188] These type of studies exemplify the combinations of diagnosis and therapeutic using QDs.

8.2.2. Theranostic Quantum Dots

The promising fluorescent properties of quantum dots provide the potential for fluorescent-guided therapies. Some quantum dots can convert energy from light to heat, leading to photothermal therapies. Chu et al. used SiO_2 coated CdTe and CdSe quantum dots as theranostic agents.[189] Fluorescence signals of quantum dots revealed their location in the tumor tissue. Upon irradiation with 671 nm laser, the tumor was ablated by photothermal phenomena. Ruan et al. conjugated a HER2 monoclonal antibody to RNase A-associated CdTe QDs for gastric cancer therapy.[190] After administration, both in vivo and ex vivo imaging showed distinguished fluorescent signals. Tumor growth was inhibited by QD treatment and the survival of tumor-bearing mice was significantly extended. QDs can also be combined with other therapeutic agents for treatments. Chou et al. conjugated quantum dots with sulfonated aluminum phthalocyanine.[191] With exposure with a 800 nm laser, energy from quantum dots can transfer to the phthalocyanine and generate cytotoxic singlet oxygen. Graphene quantum dots can also be used for PDT. Ge et al. used graphene QDs for breast cancer treatment.[183] These QDs showed strong fluorescent signals in both in vitro and in vivo studies. With laser treatment, the volume of tumors in nude mice decreased compared with control mice. Nigam et al. used albumin conjugated graphene QDs for pancreatic cancer phototreatment. In vitro, Panc-1 cells took up the graphene QDs with strong fluorescent intensity and good PDT efficiency.

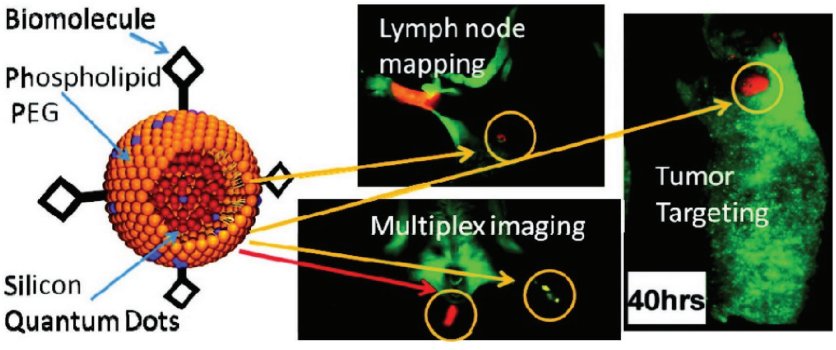

Figure 7. The left panel shows a schematic figure of phospholipid-PEG encapsulated silicon quantum dots; the right panels show NIR imaging applications including lymph node mapping, multiplex imaging and tumor specific imaging after conjugation with RGD. Reproduced with permission.[177] Copyright 2011, American Chemical Society.

8.3. Upconversion Nanoparticles (UCNPs)

8.3.1. Design of UCNPs

Upconversion luminescence (UL) is an anti-Stokes process, which is unlike the traditional Stokes one (**Figure 9**a). As shown in Figure 9b, generally, the luminescent center at ground state 1 can be pumped to excited state 1 by absorbing energy from excited photons or a corresponding energy transfer

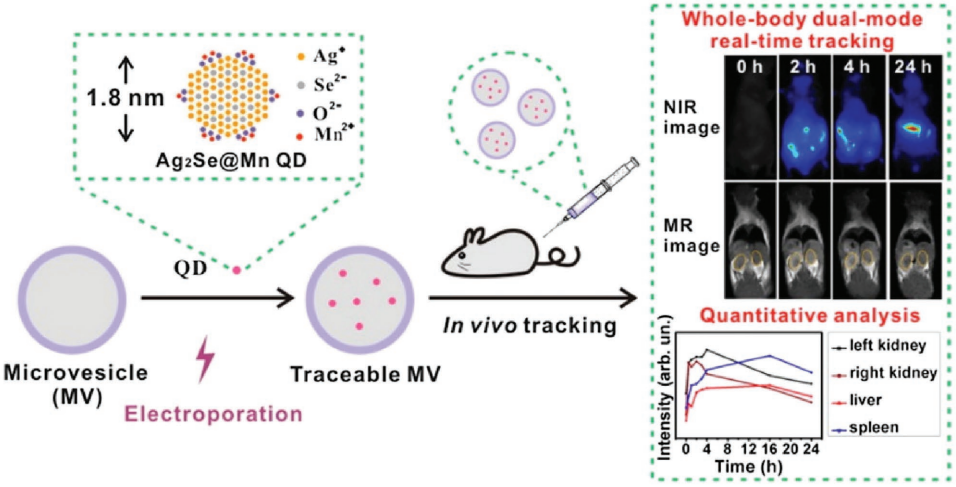

Figure 8. Ag_2Se@Mn QD labeling of cell-derived microvesicles (MVs), and their real-time dual-modality whole body monitoring and quantitative biodistribution analysis. Reproduced with permission.[187] Copyright 2016, American Chemical Society.

process. Then another excited photon or corresponding energy transfer will further promote the luminescent center to excited state 3.[192] The excited center will go back to lower-energy level by releasing high-energy emissions. The mechanism of upconversion nanoparticles is relatively complex. Currently, there are five basic theories to explain this phenomena including excited-state absorption, energy transfer upconversion, cooperative sensitization upconversion, cross relaxation and photon avalanche.[193]

UCNPs are usually dope with lanthanide elements and can have capacity to absorb NIR wavelength light and emit both UV or visible light and NIR light, as induced by UCNPs formed from Y_2O_3,[194] $NaYbF_4$,[195] and YVO_4.[196] Precise synthesis methods are important to tune the chemical and optical properties since these are affected by UCNP size, crystallization, and shape. A variety of chemical approaches have been used to create UCNPs,[193] including thermolysis (in which organometallic compounds decompose at boiling point mixed with surfactants),[197] Ostwald ripening (so that larger particles with low surface-to-volume ratio grow from energetically less stable smaller particles),[198] a hydrosolvothermal strategy (UCNPs are formed at the critical point of an organic solvent in a sealed environment),[199] or hierarchical core/shell UCNP (which is normally used in biomedical applications with the surface of UCNP coated with functional chemical compounds).[200] Most bare UCNPs are hydrophobic and toxic in biological systems and therefore surface modification is a prerequisite for in vivo applications.[201]

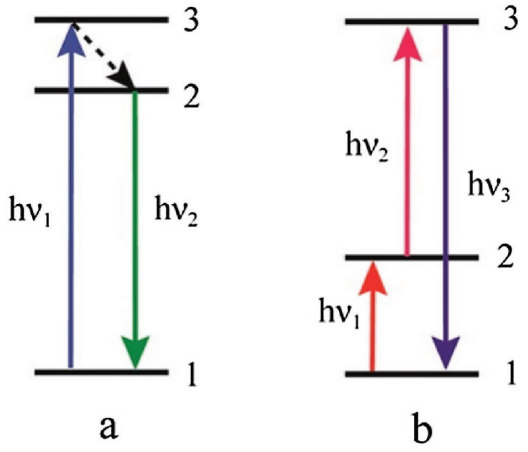

Figure 9. Schematic figure of (a) conventional photoluminescence and (b) upconversion luminescence processes. Reproduced with permission.[192] Copyright 2015, American Chemical Society.

To introduce biologically functional ligands onto UNCPs, ligand exchange is a common method that replaces the original hydrophobic UCNP surface ligands. For efficient replacement, the exchangeable ligands usually should coordinate with lanthanide ions. Surface ligands which have been reported for biological applications include poly(acrylic acid) (PAA),[202–204] hyaluronic acid (HA),[205] polyethylenimine (PEI),[206] polyethylene glycol (PEG),[207,208] polyvinylpyrrolidone (PVP),[209] phospholipids,[195,210,211] and even photosensitizers.[212,213] Other approaches include subjecting the hydrophobic outer shell (like oleic acid) to acid conditions with HCl aqueous solution,[214–216] bioconjugating the surface,[217–219] using electronic-interactions between the UCNP core and hydrophilic molecule shells,[220] surface silanization,[221] amphiphilic polymer coating,[222,223] and layer-by-layer assembly.[224,225] These methods disperse hydrophobic UCNPs into aqueous systems for biomedical applications.

Besides the commonly used 980 nm laser excitation, 808 nm excited UCNPs have been developed and this wavelength decreases water absorption of light, overcoming undesired heating effects and improving penetration depth. Recently, 808 nm excited UCNPs have been used for cancer therapy and have shown promising treatment efficiency in in vivo studies.[203,226–229]

8.3.2. UCNP Optical Imaging

Compared to conventional fluorophores, optical imaging with UCNPs has several advantages: the long wavelength excitation allows deep tissue imaging and since the emission wavelength is shorter than the excitation, there is virtually no

background autofluorescent noise.[230] Jin et al. reported interactions between the surface charge of UCNPs and mammalian cells.[206] The initial PVP-UCNPs were coated with PEI and PAA through ligand exchange and demonstrated positive and negative charge, respectively. Based on their results, by incubating with three different human cells (cervical carcinoma (HeLa), glioblastoma (U87MG), and breast carcinoma (MCF-7) cells), positively charged UCNPs enhanced cell uptake efficiency. In 2014, Zeng et al. used $NaLuF_4$:Mn/Yb/Er UCNPs to clearly map blood vessels in the lung.[216] In addition, some specific biomolecules of living cells, such as glutathione in cancer cells[214] and glycoforms on cell surface[219] were detected by UCNPs.

The upconversion of UCNPs enables them to further excite other dyes whose excitation wavelength is within an ultraviolet or visible (UV–Vis) range. This approach can overcome the otherwise low penetration depth in tissue of UV–Vis light. Several light-emitting substances have been successfully combined with UCNPs for bioimaging applications, such as D-luciferin[207] and $[Ru(dpp)_3]^{2+}Cl_2$.[221] The rapid development of UCNPs has seen interest in applying them for vivo multimodal imaging, such as combinations with PET,[222] MRI,[204,208,225] CT,[220] and PAT.[223] Recently, Rieffel et al. coated $NaYbF_4$:Tm-$NaYF_4$ UCNPs with porphyrin-phospholipid (PoP).[195] The UCNP-PoP nanoparticles were validated for six different diagnostic techniques within only one contrast agent. Lymphatic imaging was observed by upconversion, fluorescence, photoacoustic, PET, CT and Cerenkov luminescence imaging (**Figure 10**).

8.3.3. Theranostic UCNPs

UCNPs possess theranostic capacity by combining imaging function with therapeutic methods, such as PDT and chemotherapy. Many candidate photosensitizers are inefficient in vivo due to excitation wavelength in the UV–Vis range, which has low tissue penetration depth. The longer excitation wavelengths of UCNP can eliminate interference from surrounding tissues, and emission light can further excite photosensitizers for photodynamic therapy.[231] Several photosensitizers have been combined with UCNPs for photodynamic therapy such as Rose Bengal (RB),[212,213] Chlorin e6,[218,232] a trans-platinum (IV) photosensitizer,[233,234] and titanium dioxide.[235–240] In addition, by assembling UCNPs with gold-based materials, photothermal cancer therapy applications are possible.[202,228]

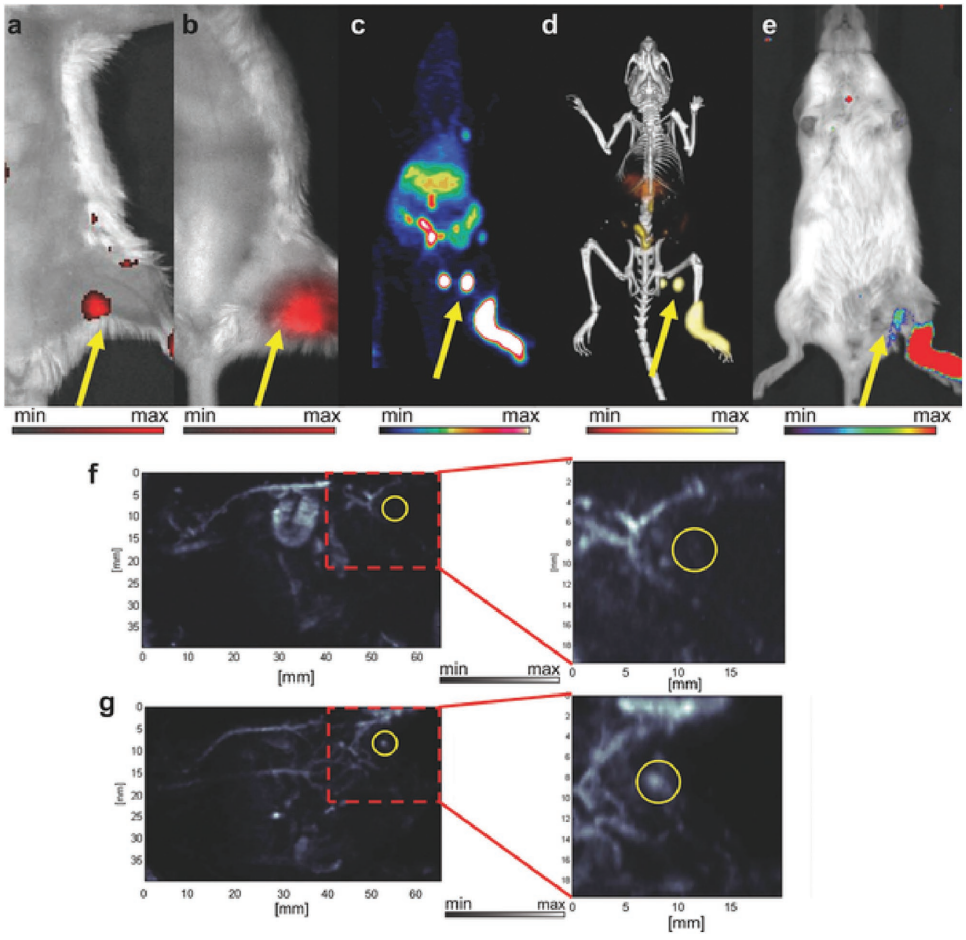

Figure 10. In vivo lymphatic imaging using porphyrin-phospholipid (PoP)-UCNPs. Accumulation of PoP-UCNPs in the first draining lymph node is indicated with yellow arrows. a) Fluorescence and b) upconversion images with the injection site cropped out of frame. c) Full body PET, d) merged PET/CT, and e) Cerenkov luminescence images. f) Photoacoustic images before and g) after injection show endogenous PA blood signal compared to the contrast enhancement that allowed visualization of the previously undetected lymph node. Reproduced with permission.[195] Copyright 2015, Wiley.

Hydrophobic interactions with hydrophobic drugs make UCNP a potential nanocarrier for image-guided chemotherapy. In 2012, Tian et al. designed PEGylated UCNPs for DOX release triggered by pH.[211] Fan et al. encapsulated cisplatin (CDDP) into UCNP-silicon nanoparticles for enhanced combination cancer therapy with combined chemotherapy and radiotherapy.[209] The complex showed better treatments to HeLa tumors than either of the two methods alone. Chien et al. thiolated DOX molecules on the surface of UCNPs through a disulfide bond could be cleaved by lysosomal enzymes for cell targeting induced release.[241] Liu et al. developed PAA coated UCNPs with pH triggered release of DOX which inhibited tumor growth.[203]

There is interest in the combination of different imaging modalities and therapeutic methods for better theranostic applications. Zeng et al. conjugated UCNPs with chlorin e6 to treat HER2-overexpressed breast cancers through PDT method.[226] This nanocomposite showed both upconversion luminescence and MRI functions. After administration, this UCNP concentrated in tumor tissue, and demonstrated distinguishable T1-weighted MRI signals even at 24 h post injection. By treatment with an 808 nm laser, this nanoparticle demonstrated more efficient fluorescence resonance energy transfer, which led to enhanced PDT. Yue et al. integrated UCNPs, Chlorin e6 and a cancer therapeutic drug TL-CPT (a thioketal linker-based ROS responsive drug) together for chemophototherapy.[242] After injection into mice for 24 h, this UCNPs still shown strong fluorescent imaging signals in organs while there were almost no fluorescent signals in the mice which treated with Chlorin e6. With laser treatment, the tumor was eliminated with no re-growth for 17 days, which was better than chemotherapy or PDT alone. Liu et al. built a multifunctional UCNPs with PDA-ICG for theranostic applications (termed as UPI).[243] With the particles, HeLa cells became fluorescent upon 980 nm laser exposure, and strong upconversion luminescence was detected after intratumoral injection of UPI. Further, the UPI successfully combined PDT and PTT together for better cancer therapeutic efficiency. Upon exposure with an 808 nm laser, UPI generated significant amounts of singlet oxygen and the temperature of treated tumors reached close to 60 °C after 200 s exposure.

8.4. Mesoporous Silica Nanoparticles

Although silica nanoparticles themselves do not provide bioimaging and therapeutic functions, their high porosity make them excellent nanocarriers. Diverse theranostic agents have been delivered by mesoporous silica nanoparticles (MSNs).

The morphology of MSNs plays a vital role for their biomedical applications. MSNs can be synthesized under basic, neutral or acidic conditions. The basic synthesis is a base-catalyzed sol–gel process, which contains two sub-reactions: hydrolysis and condensation.[244] The morphology of MSNs synthesized through the basic method is tunable but the pore size is difficult to control. In contrast, MSNs made through an acidic method can provide nanoscale MSNs with pores large enough for loading proper biomolecules.[245] Neutral synthesis methods can be used for synthesizing organic-inorganic hybrids. By changing the reaction conditions, the shapes of MSNs can be tailored into different formations. Morphological parameters such as shape[246] and size[247] affect in vivo behavior such as biodistribution and blood circulation time. Size can also impact hemolysis[248] and cellular uptake efficiency,[249] which is also influenced by aspect ratio.[250] Small sized MSNs have been reported to be superior to larger ones for delivering drugs.[251] Furthermore, for gene delivery, MSNs with large pores can adsorb nucleic acids to the inner side in case to protect them from degradation by enzymes.[252] In 2012, Sreejith et al. used ultrathin graphene oxide sheets coated with MSNs. This complex was stable and protected the contained dye from nucleophilic attack for fluorescent imaging.[253]

For theranostic purposes, several MSNs have been designed as nanocarriers with stimuli-triggered release. The cargo can selectively be released from MSNs under specific conditions. A variety of such coating materials listed in **Table 1**.

8.5. Carbon-Based Materials

8.5.1. Carbon Nanotubes (CNT)

Carbon nanotubes are one dimensional carbon nanomaterials, and are divided into single-walled carbon nanotubes (SWCNTs) and multi-walled carbon nanotubes (MWCNTs) (**Figure 11**).[271] The walls of SWCNTs and MWCNTs can be treated as a single graphene sheet, which leads to semiconducting and metallic properties. Moreover, CNTs can absorb photons within the visible and NIR-I window, and emit fluorescent signals within the NIR-II window (1000–1700 nm), and also transfer absorbed light energy to heat. Compared to shorter wavelengths, both NIR windows reduce scattering and autofluorescence for biomedical applications. Thus CNTs can be used as contrast agents

Table 1. Examples of stimuli-triggered release of MSNs.

Coating Ligands	Trigger Conditions	Delivered Materials	Functions	Reference
Aptamer modified Au nanoparticles	Aptamer specific molecules	Fluorescent dyes	Sensing	[254]
Polymers	pH, Photothermal, glutathione and Proteases	Drugs	Image-guided therapy	[255–261]
Inorganic Materials (CaP, ZnO)	pH	DOX	Cancer therapy	[262,263]
Peptides and Proteins	Redox process, pH and glutathione, proteases	Anti-cancer Drugs	Cancer therapy	[264–266]
Lipid bilayers	Endosomal disruption, photoactivation, dextrose solutions	Small interfering RNAs (siRNA), drugs	Gene delivery, Cancer therapy	[267–269]
DNA sequences	Ion-driven DNAzyme	Fluorescent dyes	Optical imaging	[270]

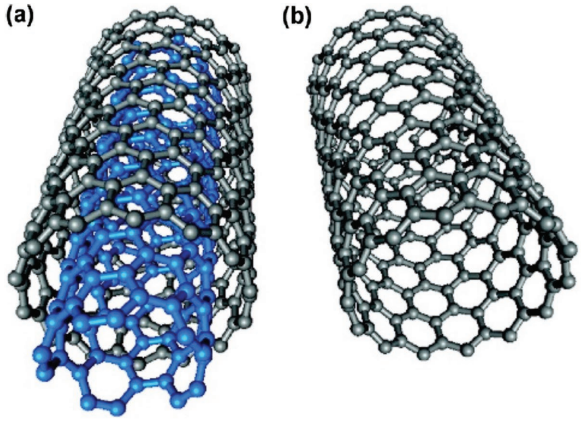

Figure 11. Schematic figure of a) MWCNT and b) SWNCT. Reproduced with permission.[271] Copyright 2009, American Chemical Society.

for optical imaging and photosensitizers for photodynamic and photothermal therapy within deeper tissues.[272] Moreover, carbon nanotubes also can be used as efficient carriers for cargo delivery.

There are several methods for synthesizing carbon nanotubes, but three which are widely used are arc discharge, chemical vapor deposition (CVD) and laser ablation.[273] Briefly, these methods aim to build carbon atom or atomic clusters and combine them again into nanotube formations. These nanotubes usually have poor solubility in aqueous systems and many organic solvents so that further modification is required before use.

The toxicity of CNTs is influenced by several parameters, such as morphology, physical and chemical properties.[274,275] The structure of CNTs allow them to easily penetrate cell membranes. Under most conditions, CNTs with longer length and larger diameters will show higher toxicity, and longer CNTs can induce inflammation and progressive fibrosis on the parietal pleura.[276] The purity of CNTs will affect biocompatibility and any metal impurities may cause toxicity. CNTs can cause adverse respiratory effects, stimulate immune responses,[277] and neuroinflammatory responses in the brain.[278] Besides toxicity, the morphology impacts the formation of surface coating and NIR II fluorescent intensity. Roxbury et al. found that single-stranded DNA chains attached strongly on the surface of small diameter SWCNTs.[279] Diao et al. found that NIR intensity of SWNTs is dependent on chirality,[280,281] which encourages the use of properly chiral CNTs[282] which can lower effective doses required.[283]

Surface coating is essential for rendering CNTs more biocompatible. CNTs can be surface-modified through covalent or noncovalent approaches, which broadens the choices of surface modification using small chemicals,[284] mesoporous silica,[285] DNA aptamers[286] or proteins.[287] CNTs can serve as therapeutic agents for anti-cancer treatment directly[288] or can encapsulate or adsorb therapeutic materials such as drugs, genes and proteins.[289]

Use of the NIR II window for optical imaging offers several advantages such as a large penetration depth, and little background. Although there are a variety of fluorophores suitable for NIR II fluorescent imaging, CNTs have shown as promise for applications including blood vessel imaging.[290] Welsher et al. used PEGylated liposomes to encapsulate single-walled carbon nanotubes for in vivo anatomical imaging.[291] Organ and fluorophore movements were clearly shown by NIR II fluorescent imaging and principal component analysis (PCA). Also this anatomical imaging ability enables for fast and long-term tumor monitoring in the NIR II window (**Figure 12**).[292,293] In 2011, Hong et al. found that gold can enhance the fluorescence of SWNTs.[294] The fluorescent uptake in U87-MG cells incubated with RGD modified SWNTs increased 9-fold after plating on gold substrates. Hong et al. dispersed SWNTs in a IR-D800 modified biocompatible surfactant.[295] After injection to the hind limb of mice and laser irradiation, the highest spatial and temporal resolution imaging of blood vessels was possible in NIR II, but not NIR I or even clinically established CT imaging. Also due to better depth penetration, this approach could quantify blood velocity in both normal and ischemic femoral arteries. Later, SWNT-IRD800 conjugates were used for brain fluorescent imaging with 1300–1400 nm emission.[296] The imaging depth could reach up to 10 mm. The reduced photon scattering allowed for microscopy in more than 2 mm depth in mice brains with sub- 10 µm resolution. These conjugates also can be used with high imaging frame rate which allows real-time dynamic recording of blood perfusion in cerebral vessels. In 2012, Iverson et al. used SWNT-coated with nitric oxide (NO)

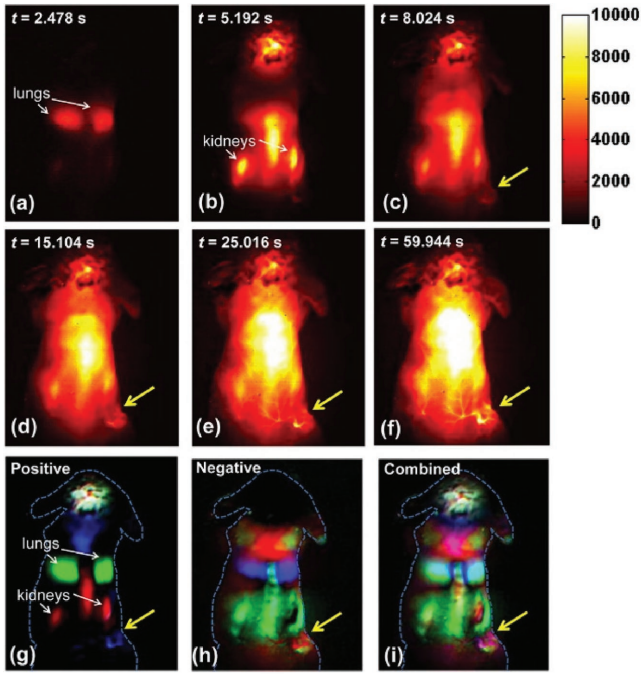

Figure 12. Dynamic NIR-II fluorescence images and contrast-enhanced images based on PCA analysis: (a–f) NIR-II fluorescence images of a 4T1 tumor bearing mouse after injection of a 200 µL solution containing 0.35 mg mL^{-1} SWNTs; (g) positive pixels from PCA, showing lungs, kidneys, and major vessels in the tumor; (h) negative pixels from PCA, showing the body of the tumor; (i) overlaid image showing the absolute value of both positive and negative pixels, from which both the vessels in the tumor and the tumor outline can be seen. Yellow arrows in the images highlight the tumor. Reproduced with permission.[292] Copyright 2012, American Chemical Society.

sensitive DNA ligated PEG for in vivo NO detection.[297] By further encapsulating alginate, the SWNTs enabled NO detection as implantable inflammation sensors and induced no adverse effects 400 days post injection. By changing the coating molecules to M13 bacteriophage, M13-SWNT could selectively image F'-negative bacteria by an attached anti-bacterial antibody.[298] Besides in vivo applications, CNTs have been used for high resolution mapping activities of single cells.[299,300] In 2014, Fakhri et al. observed a new intermediate mode of transport with the kinesin-1 motor proteins combined with SWNTs.[301]

In addition, CNTs can behave as carriers for other drugs.[302] Many drugs can be adsorbed to CNTs including DOX,[303–306] methotrexate (MTX),[307] and gemcitabine.[308] CNTs can be made to adsorb several biological molecules such as genes[309] and proteins.[310] This property enables CNTs to combine diagnosis and therapy within single CNT platform. The biodistribution and cell uptake level can be determined by imaging, and also actuate anti-cancer effects with chemotherapy.[311] Lee et al. found that when SWNTs were combined with low voltage materials, the cellular uptake efficiency could be enhanced.[312] Other studies attempted to combine magnetic nanoparticles on the surface of CNTs to form hybrids,[313] or encapsulate these magnetic nanoparticles[314,315] to track CNTs through MRI for target imaging. CNTs can also be labeled with ^{14}C for radioimaging.[316] Ren et al. used angiopep-2 modified DOX loaded multi-walled carbon nanotubes (MWNTs) to treat brain glioma.[317] Along with the accumulations of materials within brain, distinguishable brain mapping was achieved through fluorescent imaging. Mouse survival was prolonged after treatment with MWNTs. Liu et al. used PEGylated SWNTs as ca iers to deliver DOX to treat tumors.[285] Both the NIR and MRI imaging modalities can help track the materials inside the body and determine the best the time for treatment. This platform combined chemo- and phototherapy together to achieve better treatment.

Another property of CNTs is their photothermal conversion for therapeutic applications. CNTs can transfer NIR energy to heat with high efficiency, and the hollow space allows them carry one or more drugs or agents simultaneously. These advantages make CNTs an attractive photothermal contrast agent. Combining NIR imaging functions with PTT could make CNTs more efficient in cancer treatments. NIR fluorescent imaging can help monitor and map the biodistribution of CNTs, for more efficient targeted PTT treatment.[318–322] Additionally, it has been reported that MWCNTs themselves can also inhibit tumor growth.[323] Wang et al. combined Au together with single-walled carbon nanotubes (SWNTs).[324] With modification with folic acid (FA), this CNT could be uptaken in KB cells, as visualized by Raman imaging after exposure with NIR light, and also offered enhanced photothermal cancer cell kill. Wang and co-workers functionalized SWNTs with polyethylenimine (PEI) and DSPE-PEG2000-maleimide, then further loaded them with hTERT siRNA to achieve tumor-targeted siRNA delivery.[325] NIR fluorescent imaging clearly demonstrated the distribution of SWNTs inside the body, and tumors were ablated through photothermal therapy.

Sada et al. successfully used SWNT-coated dishes for cell detachment.[326] By studying HeLa cells, they found the SWNT-coated dish can not only detach large population. Also, when irradiated with an NIR laser from the bottom, the detached cell was catapulted up to top surface and kept alive. Thus, there may be unconventional approaches for CNTs for applications like cell separations.

8.5.2. Graphene Oxide

Graphene oxide (GO) is an emerging atomically thin film which is comprised of arranged carbon atoms (as shown in **Figure 13**).[327] GO demonstrates novel nanoelectronics and nanophototics, large surface area, high mechanical flexibility and chemical functionality. These features have led to an increase in GO biomedical applications during recent years.

Toxicity needs to be considered for biological applications of GO. Yang et al. found that GO is safe with ocular application.[328] Small amounts of PEGylated GO can be absorbed by the intestine after oral administration, and the materials reach the reticuloendothelial (RES) system after i.p. injection.[329] Zhang et al. found that after orally administrating reduced GO, mice showed decreased neuromuscular coordination compared to control mice.[330] GO has potential to concentrate in the lung and induce inflammation and also GO can become lodged in the kidney and not be cleared by the renal system.[331] However, the purity and oxidation level affects the behavior of GO in vivo.[332,333] GO can interfere DNA replication and induce mutagenesis in vitro, and cause formation of micronucleated polychromic erythrocytes in mice in vivo.[334] In vitro, GO can provoke blood cell aggregation.[335] Mukherjee et al. observed that GO and reduced GO induce pro-angiogenic activity.[336] GO and reduced GO could generate intracellular reactive oxygen species (ROS), which can influence the phosphorylation of Akt and active the NO signaling, thus finally triggered angiogenesis. Thus, given the concerning biological effects induced by GO itself, additional functionalization studies are required to better understand GO toxicity.

GO possesses unique optical properties. Qian et al. used PEGylated GO as a contrast agent for multi-photon imaging.[337] Clear images were generated through two-photon imaging both in vitro and in vivo. By microinjection into the brains of mice, GO nanoparticles could be discriminated with an imaging depth up to 300 μm. Moreover, GO enabled PET imaging when labeled with radioactive isotope[338,339] and could also be used for photoacoustic imaging.[340–342] GO can induce autophagy which in turn further enhances GO concentrations in cells.[343] In addition, GO has been explored for detection of specific biomolecules in vivo, such as glycosaminoglycans[344] and glucose.[345]

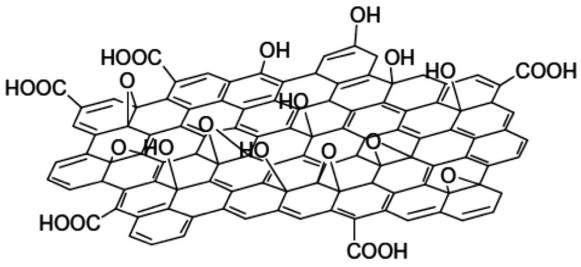

Figure 13. Schematic figure of GO. Reproduced with permission.[327] Copyright 2015, Royal Society of Chemistry.

Like carbon nanotubes, GO can absorb NIR light and convert that energy to heat for photothermal therapy, thus the combinations of NIR diagnosis and PTT functions make them great potential as theranostic agents.[346–348] With the alternations of the modified targeting materials, GO can demonstrate highly efficient photothermal therapy to specific cancers.[349] Robinson et al. conjugated RGD to reduced GO, their materials can detect cancer cells with NIR, and shown potential PTT effects.[350] Sharker et al. combined indocyanine green (ICG) with poly(PDMAEMA) modified rGO, which for pH-dependent NIR photothermal therapy.[351] By simply adjusting the surface coating materials, modified drug-loaded GO can enable triggered drug release by endogenous chemicals such as glutathione.[352] Also GO can be used as a photosensitizer for photodynamic therapy.[353]

As a nanocarrier, a wide variety of molecules have been delivered by GO, including siRNA,[354] antibodies,[355] fluorescent dyes,[356–358] peptides,[359] SPECT agents,[360] anti-tumor drugs,[348] and photosensitizers,[361] In 2015, Kim et al. conjugated IR825, PEG-g-PDMA and hyaluronic acid (HA) with GO as a pH-dependent contrast agent for cancer cell specific fluorescent imaging and photothermal therapy.[362] Huang et al. loaded Chlorin e6 onto folic acid coated GO for PDT.[363] Fluorescent imaging of cells was used to study the cell uptake, and this construct achieved effective PDT.

8.6. Porphyrin-Lipids

In general, porphyrins and related tetrapyrroles have excellent potential for theranostic applications.[364–366] In 2005, porphyrins were functionalized as building blocks of polymersomes, which improved dye stability in the carrier.[367] Later in 2011, it was shown that covalent attachment of a porphyrin to a phospholipid sidechain, resulted in formation of liposome-like nanovesicles termed porphysomes (**Figure 14**).[49] Porphysome subunits can eventually biodegrade in the liver in vivo.[368] The strong optical properties of porphysomes make them suitable for several biophotonics applications, including photothermal therapy and photoacoustic imaging. As an emerging material, porphysomes have been used for several different biomedical applications.[369] They can be used for a variety of detection modalities including US and ^{99m}Tc labeling.[370–372] Their liposome-like structure enables multiple applications as robust nanocarriers. The methodologies and modifications used for liposomes can also be applied to porphysomes to tune their stability and biological behavior. Triggered release conditions for liposomes induce triggers such as pH,[48,373] biodegradability,[374] biomolecules,[375] and thermal sensitivity.[376,377]

Porphysomes have been designed for activatable photosensitization for photodynamic therapy. Jin et al. developed porphysomes modified with folic acid to selectively target cancer cells with high expression of the folic acid receptor.[378] The initially quenched photosensitizers were unquenched upon ligand-directed cell uptake and with laser irradiation tumor growth was inhibited.

The liposome-like structure provides the possibility of dual-functionalities by combing drug delivery and phototherapy, leading to the enhanced efficacy. Carter et al. conjugated devinyl hexyloxyethy-pyropheophorbide (HPPH) with a phospholipid and encapsulated various cargos in the nanoparticle.[379] With NIR irradiation, this HPPH-lipid liposome could release loaded cargo. With DOX loading, laser treatment ablated KB tumors in mice without regrowth for at least 90 days. Light-triggered reversible opening and sealing can also be achieved at the micro-scale.[380] Recently, Luo et al. found that the light-triggered drug release speed can be controlled by adjusting the concentrations of porphyrin-phospholipid (PoP) and unsaturated lipid in the liposome, and the stability can be tuned by varying the drug-to-lipid ratio.[381,382] With only 2% PoP in a conventional long-circulating liposome formulation, blood circulation of entrapped doxorubicin was 21.9 h, and was effective for tumor photoablation relative to photodynamic therapy or chemotherapy alone.[383] Post chelation of metals into porphyrin-phospholipids can alter the phototoxicity profile.[384]

Because of the photosensitizing property of porphyrin, the porphyrin-phospholipids can also be used for image-guided photothermal therapy.[385] Muhanna et al. used pyropheophorbide-lipid porphysomes to diagnose oral carcinomas in rabbits and hamsters by photoacoustic and fluorescent imaging, and then ablated them by PTT.[386]

The porphyrin of the porphyrin-lipid conjugate is retained in the lipid bilayer. Shao et al. showed that his-tagged peptides and proteins strongly and effectively bind to the PoP liposome when they are chelated with Co(III) by capturing the tag in the hydrophobic bilayer (**Figure 15**).[387] His-tagged RGD peptides enabled pre-formed PoP liposomes to be targeted to cancer cells and this approach was also demonstrated as a potent immune adjuvant platform for his-tagged molecules.

Porphysomes and PoP can also be used for contrast agents for several imaging and diagnostic techniques, including non-linear optical microscopy,[388] fluorescent imaging,[389] Raman scattering,[390] MRI,[391,392] and PET imaging.[393,394] Rieffel et al. packaged UCNPs with PoP to readily achieve contrast imaging in six different modalities.[195] Ni et al. used porphysomes as contrast agents for tracking macrophages in a post-myocardial infarction murine model with fluorescence imaging, CT and PET.[395]

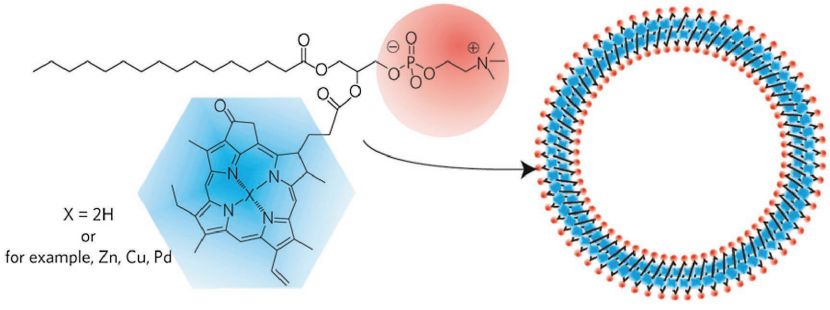

Figure 14. Schematic figure of pyropheophorbide–lipid porphysome. The phospholipid headgroup (red) and porphyrin (blue) are highlighted in the subunit (left) and assembled nanovesicle (right). Reproduced with permission.[49] Copyright 2011, Nature Publishing Group.

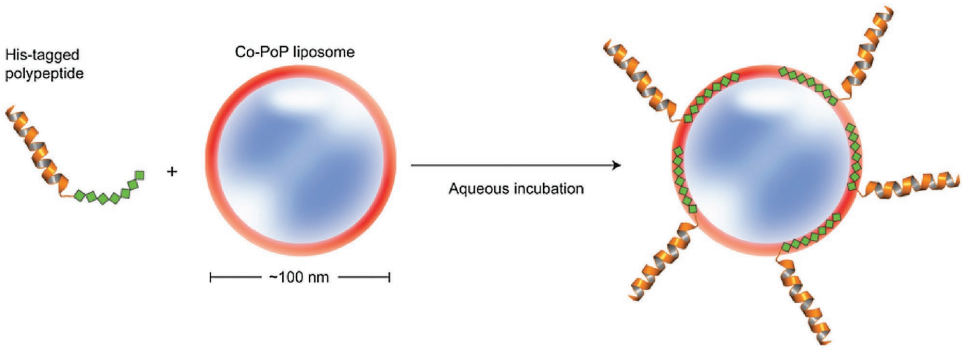

Figure 15. Schematic figure of his-tagged polypeptide insertion into Co-PoP liposomes. Reproduced with permission.[387] Copyright 2015, Nature Publishing Group.

9. Conclusion

The potential advantages offered by theranostic materials include reducing toxicity, enhancing targeting and selectivity, generating data for diagnostics and being used for therapeutic applications. Different classes of nanoparticles can be modified for biological use as contrast agents for diagnostic techniques, including MRI, PET, optical imaging, photoacoustic tomography, and CT. Recently, nanoparticles have been developed as platforms for multimodal contrast imaging. Most diagnostic imaging nanoscale agents also possess capacity for therapeutic function, which enables image-guided therapy approaches. Surface coating of nanoparticles with biocompatible molecules is required for decreasing the toxicity of theranostic agents, and provides the possibility to selectively targeting diseased areas. More research is required to improve the performance of theranostic agents, such as increasing excretion, enhancing continuous monitoring, extending blood circulation time, optimizing physiological barrier penetration, avoiding the RES, and in general start moving more of these materials into clinical trials. Thus, continuous innovations and development are needed to meet unmet clinical needs with novel theranostic approaches.

Acknowledgements

This work was supported by the National Institutes of Health (R21EB019147, R01EB017270, and DP5OD017898) and the National Science Foundation (1555220).

Received: July 12, 2016
Revised: September 9, 2016
Published online: November 7, 2016

[1] J. V. Jokerst, S. S. Gambhir, *Acc. Chem. Res.* **2011**, *44*, 1050.
[2] T. Lammers, S. Aime, W. E. Hennink, G. Storm, F. Kiessling, *Acc. Chem. Res.* **2011**, *44*, 1029.
[3] E. Huynh, G. Zheng, *WIRES: Nanomed. Nanobiotechnol.* **2013**, *5*, 250.
[4] D. Peer, J. M. Karp, S. Hong, O. C. Farokhzad, R. Margalit, R. Langer, *Nat. Nanotechnol.* **2007**, *2*, 751.
[5] S. M. Janib, A. S. Moses, J. A. MacKay, *Adv. Drug Delivery Rev.* **2010**, *62*, 1052.
[6] J. Xia, C. Kim, J. F. Lovell, *Curr. Drug Targets* **2015**, *16*, 571.
[7] D. Luo, K. A. Carter, J. F. Lovell, *WIRES: Nanomed. Nanobiotechnol.* **2015**, *7*, 169.
[8] C. Medina, M. J. Santos-Martinez, A. Radomski, O. I. Corrigan, M. W. Radomski, *Br. J. Pharmacol.* **2007**, *150*, 552.
[9] P. P. Adiseshaiah, J. B. Hall, S. E. McNeil, *WIRES: Nanomed. Nanobiotechnol.* **2010**, *2*, 99.
[10] R. Weissleder, U. Mahmood, *Radiology* **2001**, *219*, 316.
[11] D.-E. Lee, H. Koo, I.-C. Sun, J. H. Ryu, K. Kim, I. C. Kwon, *Chem. Soc. Rev.* **2012**, *41*, 2656.
[12] J. Rieffel, U. Chitgupi, J. F. Lovell, *Small* **2015**, *11*, 4445.
[13] P. Debbage, W. Jaschke, *Histochem. Cell Biol.* **2008**, *130*, 845.
[14] K. Park, S. Lee, E. Kang, K. Kim, K. Choi, I. C. Kwon, *Adv. Funct. Mater.* **2009**, *19*, 1553.
[15] S. L. Troyan, V. Kianzad, S. L. Gibbs-Strauss, S. Gioux, A. Matsui, R. Oketokoun, L. Ngo, A. Khamene, F. Azar, J. V. Frangioni, *Ann. Surg. Oncol.* **2009**, *16*, 2943.
[16] J. T. Alander, I. Kaartinen, A. Laakso, T. Pätilä, T. Spillmann, V. V. Tuchin, M. Venermo, P. Välisuo, *Int. J. Biomed. Imaging* **2012**, *2012*, 7.
[17] B. E. Schaafsma, J. S. D. Mieog, M. Hutteman, J. R. van der Vorst, P. J. K. Kuppen, C. W. G. M. Löwik, J. V. Frangioni, C. J. H. van de Velde, A. L. Vahrmeijer, *J. Surg. Oncol.* **2011**, *104*, 323.
[18] C. Richard, Q. le Masne de Chermont, D. Scherman, *Tumori* **2008**, *94*, 264.
[19] H. B. Na, I. C. Song, T. Hyeon, *Adv. Mater.* **2009**, *21*, 2133.
[20] Y.-w. Jun, J.-H. Lee, J. Cheon, *Angew. Chem., Int. Ed.* **2008**, *47*, 5122.
[21] M.-F. Bellin, *Eur. J. Radiol.* **2006**, *60*, 314.
[22] A. M. Taylor, J. R. Panting, J. Keegan, P. D. Gatehouse, D. Amin, P. Jhooti, G. Z. Yang, S. McGill, E. D. Burman, J. M. Francis, D. N. Firmin, D. J. Pennell, *J. Magn. Reson. Imaging* **1999**, *9*, 220.
[23] A. G. van der Kolk, J. Hendrikse, J. J. M. Zwanenburg, F. Visser, P. R. Luijten, *Eur. J. Radiol.* **2013**, *82*, 708.
[24] S. M. Ametamey, M. Honer, P. A. Schubiger, *Chem. Rev.* **2008**, *108*, 1501.
[25] H. Jadvar, P. M. Colletti, *Eur. J. Radiol.* **2014**, *83*, 84.
[26] J. A. Disselhorst, I. Bezrukov, A. Kolb, C. Parl, B. J. Pichler, *J. Nucl. Med.* **2014**, *55*, 2S.
[27] T. F. Massoud, S. S. Gambhir, *Genes Dev.* **2003**, *17*, 545.
[28] M. Postema, O. H. Gilja, *World J. Gastroenterol.* **2011**, *17*, 28.
[29] T. Faez, M. Emmer, K. Kooiman, M. Versluis, A. F. W. v. d. Steen, N. d. Jong, *IEEE Trans. Ultrason., Ferroelect., Freq. Control* **2013**, *60*, 1.
[30] M. Xu, L. V. Wang, *Rev. Sci. Instrum.* **2006**, *77*, 041101.
[31] C. Kim, C. Favazza, L. V. Wang, *Chem. Rev.* **2010**, *110*, 2756.
[32] L. V. Wang, S. Hu, *Science* **2012**, *335*, 1458.

[33] Y. Zhou, D. Wang, Y. Zhang, U. Chitgupi, J. Geng, Y. Wang, Y. Zhang, T. R. Cook, J. Xia, J. F. Lovell, *Theranostics* **2016**, *6*, 688.
[34] D. Luo, K. A. Carter, D. Miranda, J. F. Lovell, *Adv. Sci.* **2016**, DOI: 10.1002/advs.201600106.
[35] Y. Zhang, W. Song, J. Geng, U. Chitgupi, H. Unsal, J. Federizon, J. Rzayev, D. K. Sukumaran, P. Alexandridis, J. F. Lovell, *Nat. Commun.* **2016**, *7*, 11649.
[36] S. Jelveh, D. B. Chithrani, *Cancers (Basel)* **2011**, *3*, 1081.
[37] A. M. Alkilany, L. B. Thompson, S. P. Boulos, P. N. Sisco, C. J. Murphy, *Adv. Drug Delivery Rev.* **2012**, *64*, 190.
[38] K. Yang, L. Feng, X. Shi, Z. Liu, *Chem. Soc. Rev.* **2013**, *42*, 530.
[39] L. Cheng, K. Yang, Q. Chen, Z. Liu, *ACS Nano* **2012**, *6*, 5605.
[40] L. Xu, L. Cheng, C. Wang, R. Peng, Z. Liu, *Polym. Chem.* **2014**, *5*, 1573.
[41] V. P. Torchilin, *Nat. Rev. Drug Discovery* **2005**, *4*, 145.
[42] H.-I. Chang, M.-K. Yeh, *Int. J. Nanomedicine* **2012**, *7*.
[43] T. M. Allen, P. R. Cullis, *Adv. Drug Delivery Rev.* **2013**, *65*, 36.
[44] F. Emmetiere, C. Irwin, N. T. Viola-Villegas, V. Longo, S. M. Cheal, P. Zanzonico, N. Pillarsetty, W. A. Weber, J. S. Lewis, T. Reiner, *Bioconjugate Chem.* **2013**, *24*, 1784.
[45] H. Xing, L. Tang, X. Yang, K. Hwang, W. Wang, Q. Yin, N. Y. Wong, L. W. Dobrucki, N. Yasui, J. A. Katzenellenbogen, W. G. Helferich, J. Cheng, Y. Lu, *J. Mater. Chem. B* **2013**, *1*, 5288.
[46] G. Kibria, H. Hatakeyama, N. Ohga, K. Hida, H. Harashima, *J. Controlled Release* **2011**, *153*, 141.
[47] T. Ta, T. M. Porter, *J. Controlled Release* **2013**, *169*, 112.
[48] R. Nahire, R. Hossain, R. Patel, S. Paul, V. Meghnani, A. H. Ambre, K. N. Gange, K. S. Katti, E. Leclerc, D. K. Srivastava, K. Sarkar, S. Mallik, *Mol. Pharm.* **2014**, *11*, 4059.
[49] J. F. Lovell, C. S. Jin, E. Huynh, H. Jin, C. Kim, J. L. Rubinstein, W. C. W. Chan, W. Cao, L. V. Wang, G. Zheng, *Nat. Mater.* **2011**, *10*, 324.
[50] J.-F. Gohy, Y. Zhao, *Chem. Soc. Rev.* **2013**, *42*, 7117.
[51] K. Miyata, R. J. Christie, K. Kataoka, *React. Funct. Polym.* **2011**, *71*, 227.
[52] Y. Zhang, M. Jeon, L. J. Rich, H. Hong, J. Geng, Y. Zhang, S. Shi, T. E. Barnhart, P. Alexandridis, J. D. Huizinga, M. Seshadri, W. Cai, C. Kim, J. F. Lovell, *Nat. Nanotechnol.* **2014**, *9*, 631.
[53] Y. Zhang, D. Wang, S. Goel, B. Sun, U. Chitgupi, J. Geng, H. Sun, T. E. Barnhart, W. Cai, J. Xia, J. F. Lovell, *Adv. Mater.* **2016**, n/a.
[54] A. Surendiran, S. Sandhiya, S. Pradhan, C. Adithan, *Indian J. Med. Res.* **2009**, *130*.
[55] C. C. Lee, J. A. MacKay, J. M. J. Frechet, F. C. Szoka, *Nat. Biotechnol.* **2005**, *23*, 1517.
[56] S. Svenson, D. A. Tomalia, *Adv. Drug Delivery Rev.* **2012**, *64*, Supplement, 102.
[57] S. Vardharajula, S. Z. Ali, P. M. Tiwari, E. Eroğlu, K. Vig, V. A. Dennis, S. R. Singh, *Int. J. Nanomedicine* **2012**, *7*, 5361.
[58] H. Gong, R. Peng, Z. Liu, *Adv. Drug Delivery Rev.* **2013**, *65*, 1951.
[59] D. Bitounis, H. Ali-Boucetta, B. H. Hong, D.-H. Min, K. Kostarelos, *Adv. Mater.* **2013**, *25*, 2258.
[60] C. Chung, Y.-K. Kim, D. Shin, S.-R. Ryoo, B. H. Hong, D.-H. Min, *Acc. Chem. Res.* **2013**, *46*, 2211.
[61] M. A. Miller, S. Gadde, C. Pfirschke, C. Engblom, M. M. Sprachman, R. H. Kohler, K. S. Yang, A. M. Laughney, G. Wojtkiewicz, N. Kamaly, S. Bhonagiri, M. J. Pittet, O. C. Farokhzad, R. Weissleder, *Sci. Transl. Med.* **2015**, *7*, 314ra183.
[62] K. Luyts, D. Napierska, B. Nemery, P. H. M. Hoet, *Env. Sci. Process. Impact* **2013**, *15*, 23.
[63] A. Nel, T. Xia, L. Mädler, N. Li, *Science* **2006**, *311*, 622.
[64] S. Sharifi, S. Behzadi, S. Laurent, M. Laird Forrest, P. Stroeve, M. Mahmoudi, *Chem. Soc. Rev.* **2012**, *41*, 2323.
[65] S. A. Love, M. A. Maurer-Jones, J. W. Thompson, Y.-S. Lin, C. L. Haynes, *Annu. Rev. Anal. Chem.* **2012**, *5*, 181.
[66] N. Leibman, J. A. McKnight, *Clin. Tech. Small Anim. Pract.* **2003**, *18*, 67.
[67] E.-K. Lim, T. Kim, S. Paik, S. Haam, Y.-M. Huh, K. Lee, *Chem. Rev.* **2015**, *115*, 327.
[68] D. E. Owens III, N. A. Peppas, *Int. J. Pharm.* **2006**, *307*, 93.
[69] H. S. Choi, W. Liu, P. Misra, E. Tanaka, J. P. Zimmer, B. Itty Ipe, M. G. Bawendi, J. V. Frangioni, *Nat. Biotechnol.* **2007**, *25*, 1165.
[70] H. Huang, R. Hernandez, J. Geng, H. Sun, W. Song, F. Chen, S. A. Graves, R. J. Nickles, C. Cheng, W. Cai, J. F. Lovell, *Biomaterials* **2016**, *76*, 25.
[71] J. Nicolas, S. Mura, D. Brambilla, N. Mackiewicz, P. Couvreur, *Chem. Soc. Rev.* **2013**, *42*, 1147.
[72] C. Sun, J. S. H. Lee, M. Zhang, *Adv. Drug Delivery Rev.* **2008**, *60*, 1252.
[73] T. Pedro, M. M. del Puerto, V.-V. Sabino, G.-C. Teresita, J. S. Carlos, *J. Phys. D: Appl. Phys.* **2003**, *36*, R182.
[74] L. H. Reddy, J. L. Arias, J. Nicolas, P. Couvreur, *Chem. Rev.* **2012**, *112*, 5818.
[75] J. D. G. Durán, J. L. Arias, V. Gallardo, A. V. Delgado, *J. Pharm. Sci.* **2008**, *97*, 2948.
[76] A.-H. Lu, E. L. Salabas, F. Schüth, *Angew. Chem., Int. Ed.* **2007**, *46*, 1222.
[77] T.-H. Shin, Y. Choi, S. Kim, J. Cheon, *Chem. Soc. Rev.* **2015**, *44*, 4501.
[78] R. Thomas, I.-K. Park, Y. Y. Jeong, *Int. J. Mol. Sci.* **2013**, *14*, 15910.
[79] M. F. Kircher, A. de la Zerda, J. V. Jokerst, C. L. Zavaleta, P. J. Kempen, E. Mittra, K. Pitter, R. Huang, C. Campos, F. Habte, R. Sinclair, C. W. Brennan, I. K. Mellinghoff, E. C. Holland, S. S. Gambhir, *Nat. Med.* **2012**, *18*, 829.
[80] A. Neuwelt, N. Sidhu, C.-A. A. Hu, G. Mlady, S. C. Eberhardt, L. O. Sillerud, *AJR Am. J. Roentgenol.* **2015**, *204*, W302.
[81] M. Mahmoudi, S. Sant, B. Wang, S. Laurent, T. Sen, *Adv. Drug Delivery Rev.* **2011**, *63*, 24.
[82] D. Liu, W. Wu, J. Ling, S. Wen, N. Gu, X. Zhang, *Adv. Funct. Mater.* **2011**, *21*, 1498.
[83] B. H. Kim, N. Lee, H. Kim, K. An, Y. I. Park, Y. Choi, K. Shin, Y. Lee, S. G. Kwon, H. B. Na, J.-G. Park, T.-Y. Ahn, Y.-W. Kim, W. K. Moon, S. H. Choi, T. Hyeon, *J. Am. Chem. Soc.* **2011**, *133*, 12624.
[84] H. K. Patra, N. U. Khaliq, T. Romu, E. Wiechec, M. Borga, A. P. F. Turner, A. Tiwari, *Adv. Healthcare Mater.* **2014**, *3*, 526.
[85] H. Xie, Y. Zhu, W. Jiang, Q. Zhou, H. Yang, N. Gu, Y. Zhang, H. Xu, H. Xu, X. Yang, *Biomaterials* **2011**, *32*, 495.
[86] Y. Song, Z. Huang, J. Xu, D. Ren, Y. Wang, X. Zheng, Y. Shen, L. Wang, H. Gao, J. Hou, Z. Pang, J. Qian, J. Ge, *Biomaterials* **2014**, *35*, 2961.
[87] M. K. Yu, D. Kim, I.-H. Lee, J.-S. So, Y. Y. Jeong, S. Jon, *Small* **2011**, *7*, 2241.
[88] H. Wei, N. Insin, J. Lee, H.-S. Han, J. M. Cordero, W. Liu, M. G. Bawendi, *Nano Lett.* **2012**, *12*, 22.
[89] R. T. M. de Rosales, R. Tavaré, R. L. Paul, M. Jauregui-Osoro, A. Protti, A. Glaria, G. Varma, I. Szanda, P. J. Blower, *Angew. Chem., Int. Ed.* **2011**, *50*, 5509.
[90] R. Chakravarty, H. F. Valdovinos, F. Chen, C. M. Lewis, P. A. Ellison, H. Luo, M. E. Meyerand, R. J. Nickles, W. Cai, *Adv. Mater.* **2014**, *26*, 5119.
[91] H. Yang, Y. Zhuang, Y. Sun, A. Dai, X. Shi, D. Wu, F. Li, H. Hu, S. Yang, *Biomaterials* **2011**, *32*, 4584.
[92] J. Hu, Y. Qian, X. Wang, T. Liu, S. Liu, *Langmuir* **2012**, *28*, 2073.
[93] V. P. Torchilin, *Nat. Rev. Drug Discovery* **2014**, *13*, 813.
[94] L. Ao, B. Wang, P. Liu, L. Huang, C. Yue, D. Gao, C. Wu, W. Su, *Nanoscale* **2014**, *6*, 10710.
[95] D. Vyas, N. Lopez-Hisijos, S. Gandhi, M. El-Dakdouki, M. D. Basson, M. F. Walsh, X. Huang, A. K. Vyas, L. S. Chaturvedi, *J. Nanosci. Nanotechnol.* **2015**, *15*, 6413.

[96] H. Jeon, J. Kim, Y. M. Lee, J. Kim, H. W. Choi, J. Lee, H. Park, Y. Kang, I.-S. Kim, B.-H. Lee, A. S. Hoffman, W. J. Kim, *J. Controlled Release* **2016**, *231*, 68.
[97] L. Xiao, J. Li, D. F. Brougham, E. K. Fox, N. Feliu, A. Bushmelev, A. Schmidt, N. Mertens, F. Kiessling, M. Valldor, B. Fadeel, S. Mathur, *ACS Nano* **2011**, *5*, 6315.
[98] U. I. Tromsdorf, O. T. Bruns, S. C. Salmen, U. Beisiegel, H. Weller, *Nano Lett.* **2009**, *9*, 4434.
[99] L.-h. Shen, J.-f. Bao, D. Wang, Y.-x. Wang, Z.-w. Chen, L. Ren, X. Zhou, X.-b. Ke, M. Chen, A.-q. Yang, *Nanoscale* **2013**, *5*, 2133.
[100] L. Zeng, W. Ren, J. Zheng, P. Cui, A. Wu, *PCCP* **2012**, *14*, 2631.
[101] J. Ruiz-Cabello, B. P. Barnett, P. A. Bottomley, J. W. M. Bulte, *NMR Biomed.* **2011**, *24*, 114.
[102] E. T. Ahrens, J. Zhong, *NMR Biomed.* **2013**, *26*, 860.
[103] M. S. Fox, J. M. Gaudet, P. J. Foster, *Magn. Reson. Insights* **2015**, *8*, 53.
[104] A. Keliris, I. Mamedov, G. E. Hagberg, N. K. Logothetis, K. Scheffler, J. Engelmann, *Contrast Media Mol. Imaging* **2012**, *7*, 478.
[105] D. K. Kadayakkara, S. Ranganathan, W.-B. Young, E. T. Ahrens, *Lab. Invest.* **2012**, *92*, 636.
[106] S. Temme, F. Bönner, J. Schrader, U. Flögel, *WIRES: Nanomed. Nanobiotechnol.* **2012**, *4*, 329.
[107] J. Zhong, P. H. Mills, T. K. Hitchens, E. T. Ahrens, *Magn. Reson. Med.* **2013**, *69*, 1683.
[108] G. Weise, T. C. Basse-Lüsebrink, C. Kleinschnitz, T. Kampf, P. M. Jakob, G. Stoll, *PLoS One* **2011**, *6*, 1.
[109] A. Balducci, B. M. Helfer, E. T. Ahrens, C. F. O'Hanlon III, A. K. Wesa, *J. Inflamm.* **2012**, *9*, 24.
[110] L. Mignion, J. Magat, O. Schakman, E. Marbaix, B. Gallez, B. F. Jordan, *Magn. Reson. Med.* **2013**, *69*, 248.
[111] M. Botta, L. Tei, *Eur. J. Inorg. Chem.* **2012**, *2012*, 1945.
[112] C.-T. Yang, K.-H. Chuang, *MedChemComm* **2012**, *3*, 552.
[113] L. Telgmann, M. Sperling, U. Karst, *Anal. Chim. Acta* **2013**, *764*, 1.
[114] J. L. Vivero-Escoto, K. M. L. Taylor-Pashow, R. C. Huxford, J. D. Rocca, C. Okoruwa, H. An, W. Lin, W. Lin, *Small* **2011**, *7*, 3519.
[115] M. Cao, P. Wang, Y. Kou, J. Wang, J. Liu, Y. Li, J. Li, L. Wang, C. Chen, *ACS Appl. Mater. Interfaces* **2015**, *7*, 25014.
[116] C. E. Smith, A. Shkumatov, S. G. Withers, B. Yang, J. F. Glockner, S. Misra, E. J. Roy, C.-H. Wong, S. C. Zimmerman, H. Kong, *ACS Nano* **2013**, *7*, 9599.
[117] T. Courant, V. G. Roullin, C. Cadiou, M. Callewaert, M. C. Andry, C. Portefaix, C. Hoeffel, M. C. de Goltstein, M. Port, S. Laurent, L. V. Elst, R. Muller, M. Molinari, F. Chuburu, *Angew. Chem., Int. Ed.* **2012**, *51*, 9119.
[118] J. Lim, B. Turkbey, M. Bernardo, L. H. Bryant, M. Garzoni, G. M. Pavan, T. Nakajima, P. L. Choyke, E. E. Simanek, H. Kobayashi, *Bioconjugate Chem.* **2012**, *23*, 2291.
[119] W. C. Floyd, P. J. Klemm, D. E. Smiles, A. C. Kohlgruber, V. C. Pierre, J. L. Mynar, J. M. J. Fréchet, K. N. Raymond, *J. Am. Chem. Soc.* **2011**, *133*, 2390.
[120] F. Arena, J. B. Singh, E. Gianolio, R. Stefanìa, S. Aime, *Bioconjugate Chem.* **2011**, *22*, 2625.
[121] T. Yamane, K. Hanaoka, Y. Muramatsu, K. Tamura, Y. Adachi, Y. Miyashita, Y. Hirata, T. Nagano, *Bioconjugate Chem.* **2011**, *22*, 2227.
[122] L. N. Goswami, L. Ma, S. Chakravarty, Q. Cai, S. S. Jalisatgi, M. F. Hawthorne, *Inorg. Chem.* **2013**, *52*, 1694.
[123] D. Ye, A. J. Shuhendler, P. Pandit, K. D. Brewer, S. S. Tee, L. Cui, G. Tikhomirov, B. Rutt, J. Rao, *Chem. Sci.* **2014**, *5*, 3845.
[124] D. Pan, A. H. Schmieder, S. A. Wickline, G. M. Lanza, *Tetrahedron* **2011**, *67*, 8431.
[125] D. Bissig, B. A. Berkowitz, *Neuroimage* **2011**, *58*, 749.
[126] K. C. Chan, J. Li, P. Kau, I. Y. Zhou, M. M. Cheung, C. Lau, J. Yang, K.-f. So, E. X. Wu, *Neuroimage* **2011**, *54*, 389.
[127] K. C. Chan, S.-J. Fan, R. W. Chan, J. S. Cheng, I. Y. Zhou, E. X. Wu, *Neuroimage* **2014**, *90*, 235.
[128] N. Just, R. Gruetter, *NMR Biomed.* **2011**, *24*, 1326.
[129] S. Hasegawa, M. Koshikawa-Yano, S. Saito, Y. Morokoshi, T. Furukawa, I. Aoki, T. Saga, *Int. J. Cancer* **2011**, *128*, 2138.
[130] I. Szabo, S. G. Crich, D. Alberti, F. K. Kalman, S. Aime, *Chem. Commun.* **2012**, *48*, 2436.
[131] J. Kim, I.-Y. Choi, M. L. Michaelis, P. Lee, *Neuroimage* **2011**, *56*, 1286.
[132] K. C. Briley-Saebo, T. H. Nguyen, A. M. Saeboe, Y.-S. Cho, S. K. Ryu, E. Volkava, S. Dickson, G. Leibundgut, P. Weisner, S. Green, F. Casanada, Y. I. Miller, W. Shaw, J. L. Witztum, Z. A. Fayad, S. Tsimikas, *J. Am. Coll. Cardiol.* **2012**, *59*, 616.
[133] S. Dedeurwaerdere, K. Fang, M. Chow, Y. T. Shen, I. Noordman, L. van Raay, N. Faggian, M. Porritt, G. F. Egan, T. J. O'Brien, *Neuroimage* **2013**, *68*, 30.
[134] N. V. Malkova, J. J. Gallagher, C. Z. Yu, R. E. Jacobs, P. H. Patterson, *Proc. Natl. Acad. Sci. USA* **2014**, *111*, E2492.
[135] C. M. Lewis, S. A. Graves, R. Hernandez, H. F. Valdovinos, T. E. Barnhart, W. Cai, M. E. Meyerand, R. J. Nickles, M. Suzuki, *Theranostics* **2015**, *5*, 227.
[136] C. S. S. R. Kumar, F. Mohammad, *Adv. Drug Delivery Rev.* **2011**, *63*, 789.
[137] B. Mehdaoui, A. Meffre, J. Carrey, S. Lachaize, L.-M. Lacroix, M. Gougeon, B. Chaudret, M. Respaud, *Adv. Funct. Mater.* **2011**, *21*, 4573.
[138] R. Ghosh, L. Pradhan, Y. P. Devi, S. S. Meena, R. Tewari, A. Kumar, S. Sharma, N. S. Gajbhiye, R. K. Vatsa, B. N. Pandey, R. S. Ningthoujam, *J. Mater. Chem.* **2011**, *21*, 13388.
[139] F. Gao, Z. Yan, J. Zhou, Y. Cai, J. Tang, *J. Nanopart. Res.* **2012**, *14*, 1.
[140] N. V. Jadhav, A. I. Prasad, A. Kumar, R. Mishra, S. Dhara, K. R. Babu, C. L. Prajapat, N. L. Misra, R. S. Ningthoujam, B. N. Pandey, R. K. Vatsa, *Colloids Surf. B Biointerfaces* **2013**, *108*, 158.
[141] E. Fantechi, C. Innocenti, M. Zanardelli, M. Fittipaldi, E. Falvo, M. Carbo, V. Shullani, L. Di Cesare Mannelli, C. Ghelardini, A. M. Ferretti, A. Ponti, C. Sangregorio, P. Ceci, *ACS Nano* **2014**, *8*, 4705.
[142] J. Ruan, J. Ji, H. Song, Q. Qian, K. Wang, C. Wang, D. Cui, *Nanoscale Res. Lett.* **2012**, *7*, 1.
[143] H. S. Huang, J. F. Hainfeld, *Int. J. Nanomedicine* **2013**, *8*, 2521.
[144] Q. L. Jiang, S. W. Zheng, R. Y. Hong, S. M. Deng, L. Guo, R. L. Hu, B. Gao, M. Huang, L. F. Cheng, G. H. Liu, Y. Q. Wang, *Appl. Surf. Sci.* **2014**, *307*, 224.
[145] R. Di Corato, G. Béalle, J. Kolosnjaj-Tabi, A. Espinosa, O. Clément, A. K. A. Silva, C. Ménager, C. Wilhelm, *ACS Nano* **2015**, *9*, 2904.
[146] M. Chu, Y. Shao, J. Peng, X. Dai, H. Li, Q. Wu, D. Shi, *Biomaterials* **2013**, *34*, 4078.
[147] S. Shen, S. Wang, R. Zheng, X. Zhu, X. Jiang, D. Fu, W. Yang, *Biomaterials* **2015**, *39*, 67.
[148] A. Espinosa, R. Di Corato, J. Kolosnjaj-Tabi, P. Flaud, T. Pellegrino, C. Wilhelm, *ACS Nano* **2016**, *10*, 2436.
[149] Y. Zhu, C. Tao, *RSC Adv.* **2015**, *5*, 22365.
[150] P. T. Yin, S. Shah, N. J. Pasquale, O. B. Garbuzenko, T. Minko, K.-B. Lee, *Biomaterials* **2016**, *81*, 46.
[151] D. Yoo, J.-H. Lee, T.-H. Shin, J. Cheon, *Acc. Chem. Res.* **2011**, *44*, 863.
[152] D. Ho, X. Sun, S. Sun, *Acc. Chem. Res.* **2011**, *44*, 875.
[153] N. Schleich, P. Sibret, P. Danhier, B. Ucakar, S. Laurent, R. N. Muller, C. Jérôme, B. Gallez, V. Préat, F. Danhier, *Int. J. Pharm.* **2013**, *447*, 94.
[154] F. Dilnawaz, A. Singh, S. Mewar, U. Sharma, N. R. Jagannathan, S. K. Sahoo, *Biomaterials* **2012**, *33*, 2936.
[155] S.-F. Lee, X.-M. Zhu, Y.-X. J. Wang, S.-H. Xuan, Q. You, W.-H. Chan, C.-H. Wong, F. Wang, J. C. Yu, C. H. K. Cheng, K. C.-F. Leung, *ACS Appl. Mater. Interfaces* **2013**, *5*, 1566.

[156] J. S. Basuki, H. T. T. Duong, A. Macmillan, R. B. Erlich, L. Esser, M. C. Akerfeldt, R. M. Whan, M. Kavallaris, C. Boyer, T. P. Davis, *ACS Nano* **2013**, *7*, 10175.
[157] C. Wang, S. Ravi, U. S. Garapati, M. Das, M. Howell, J. Mallela, S. Alwarappan, S. S. Mohapatra, S. Mohapatra, *J. Mater. Chem. B* **2013**, *1*, 4396.
[158] G. Y. Lee, W. P. Qian, L. Wang, Y. A. Wang, C. A. Staley, M. Satpathy, S. Nie, H. Mao, L. Yang, *ACS Nano* **2013**, *7*, 2078.
[159] X.-R. Song, X. Wang, S.-X. Yu, J. Cao, S.-H. Li, J. Li, G. Liu, H.-H. Yang, X. Chen, *Adv. Mater.* **2015**, *27*, 3285.
[160] Z. Zhou, Y. Sun, J. Shen, J. Wei, C. Yu, B. Kong, W. Liu, H. Yang, S. Yang, W. Wang, *Biomaterials* **2014**, *35*, 7470.
[161] K. Hayashi, M. Nakamura, W. Sakamoto, T. Yogo, H. Miki, S. Ozaki, M. Abe, T. Matsumoto, K. Ishimura, *Theranostics* **2013**, *3*, 366.
[162] J. Yu, C. Yang, J. Li, Y. Ding, L. Zhang, M. Z. Yousaf, J. Lin, R. Pang, L. Wei, L. Xu, F. Sheng, C. Li, G. Li, L. Zhao, Y. Hou, *Adv. Mater.* **2014**, *26*, 4114.
[163] L. Shao, Y. Gao, F. Yan, *Sensors* **2011**, *11*, 11736.
[164] K. S. Krishna, Y. Li, S. Li, C. S. S. R. Kumar, *Adv. Drug Delivery Rev.* **2013**, *65*, 1470.
[165] A. Mukherjee, Y. Shim, J. Myong Song, *Biotechnol. J.* **2016**, *11*, 31.
[166] Y. Wang, L. Chen, *Nanomed Nanotech. Biol. Med.* **2011**, *7*, 385.
[167] M. Bruchez, M. Moronne, P. Gin, S. Weiss, A. P. Alivisatos, *Science* **1998**, *281*, 2013.
[168] W. C. W. Chan, S. Nie, *Science* **1998**, *281*, 2016.
[169] S. J. Rosenthal, J. C. Chang, O. Kovtun, J. R. McBride, I. D. Tomlinson, *Chem. Biol.* **2011**, *18*, 10.
[170] K. D. Wegner, N. Hildebrandt, *Chem. Soc. Rev.* **2015**, *44*, 4792.
[171] H.-H. Wang, C.-A. J. Lin, C.-H. Lee, Y.-C. Lin, Y.-M. Tseng, C.-L. Hsieh, C.-H. Chen, C.-H. Tsai, C.-T. Hsieh, J.-L. Shen, W.-H. Chan, W. H. Chang, H.-I. Yeh, *ACS Nano* **2011**, *5*, 4337.
[172] G. Ma, *ACS Appl. Mater. Interfaces* **2013**, *5*, 2835.
[173] Y. Zhang, G. Hong, Y. Zhang, G. Chen, F. Li, H. Dai, Q. Wang, *ACS Nano* **2012**, *6*, 3695.
[174] G. Hong, J. T. Robinson, Y. Zhang, S. Diao, A. L. Antaris, Q. Wang, H. Dai, *Angew. Chem.* **2012**, *124*, 9956.
[175] C. Li, Y. Zhang, M. Wang, Y. Zhang, G. Chen, L. Li, D. Wu, Q. Wang, *Biomaterials* **2014**, *35*, 393.
[176] P. Pierobon, G. Cappello, *Adv. Drug Delivery Rev.* **2012**, *64*, 167.
[177] F. Erogbogbo, K.-T. Yong, I. Roy, R. Hu, W.-C. Law, W. Zhao, H. Ding, F. Wu, R. Kumar, M. T. Swihart, P. N. Prasad, *ACS Nano* **2011**, *5*, 413.
[178] X. Sun, X. Huang, J. Guo, W. Zhu, Y. Ding, G. Niu, A. Wang, D. O. Kiesewetter, Z. L. Wang, S. Sun, X. Chen, *J. Am. Chem. Soc.* **2014**, *136*, 1706.
[179] A. J. Shuhendler, P. Prasad, H.-K. C. Chan, C. R. Gordijo, B. Soroushian, M. Kolios, K. Yu, P. J. O'Brien, A. M. Rauth, X. Y. Wu, *ACS Nano* **2011**, *5*, 1958.
[180] P. Subramaniam, S. J. Lee, S. Shah, S. Patel, V. Starovoytov, K.-B. Lee, *Adv. Mater.* **2012**, *24*, 4014.
[181] J. S. Park, S. W. Yi, H. J. Kim, S. M. Kim, S. H. Shim, K.-H. Park, *Biomaterials* **2016**, *77*, 14.
[182] C.-J. Wen, L.-W. Zhang, S. A. Al-Suwayeh, T.-C. Yen, J.-Y. Fang, *Int. J. Nanomedicine* **2012**, *7*, 1599.
[183] J. Ge, M. Lan, B. Zhou, W. Liu, L. Guo, H. Wang, Q. Jia, G. Niu, X. Huang, H. Zhou, X. Meng, P. Wang, C.-S. Lee, W. Zhang, X. Han, *Nat. Commun.* **2014**, 5.
[184] E. S. Shibu, K. Ono, S. Sugino, A. Nishioka, A. Yasuda, Y. Shigeri, S.-i. Wakida, M. Sawada, V. Biju, *ACS Nano* **2013**, *7*, 9851.
[185] H.-S. Han, E. Niemeyer, Y. Huang, W. S. Kamoun, J. D. Martin, J. Bhaumik, Y. Chen, S. Roberge, J. Cui, M. R. Martin, D. Fukumura, R. K. Jain, M. G. Bawendi, D. G. Duda, *Proc. Natl. Acad. Sci. USA* **2015**, *112*, 1350.
[186] D. Gao, P. Zhang, Z. Sheng, D. Hu, P. Gong, C. Chen, Q. Wan, G. Gao, L. Cai, *Adv. Funct. Mater.* **2014**, *24*, 3897.
[187] J.-Y. Zhao, G. Chen, Y.-P. Gu, R. Cui, Z.-L. Zhang, Z.-L. Yu, B. Tang, Y.-F. Zhao, D.-W. Pang, *J. Am. Chem. Soc.* **2016**, *138*, 1893.
[188] Y. Yong, X. Cheng, T. Bao, M. Zu, L. Yan, W. Yin, C. Ge, D. Wang, Z. Gu, Y. Zhao, *ACS Nano* **2015**, *9*, 12451.
[189] M. Chu, X. Pan, D. Zhang, Q. Wu, J. Peng, W. Hai, *Biomaterials* **2012**, *33*, 7071.
[190] J. Ruan, H. Song, Q. Qian, C. Li, K. Wang, C. Bao, D. Cui, *Biomaterials* **2012**, *33*, 7093.
[191] K.-L. Chou, N. Won, J. Kwag, S. Kim, J.-Y. Chen, *J. Mater. Chem. B* **2013**, *1*, 4584.
[192] J. Zhou, Q. Liu, W. Feng, Y. Sun, F. Li, *Chem. Rev.* **2015**, *115*, 395.
[193] G. Chen, H. Qiu, P. N. Prasad, X. Chen, *Chem. Rev.* **2014**, *114*, 5161.
[194] Y. Onodera, T. Nunokawa, O. Odawara, H. Wada, *J. Lumin.* **2013**, *137*, 220.
[195] J. Rieffel, F. Chen, J. Kim, G. Chen, W. Shao, S. Shao, U. Chitgupi, R. Hernandez, S. A. Graves, R. J. Nickles, P. N. Prasad, C. Kim, W. Cai, J. F. Lovell, *Adv. Mater.* **2015**, *27*, 1785.
[196] Y. Liang, P. Chui, X. Sun, Y. Zhao, F. Cheng, K. Sun, *J. Alloys Compd.* **2013**, *552*, 289.
[197] W. Niu, S. Wu, S. Zhang, J. Li, L. Li, *Dalton Trans.* **2011**, *40*, 3305.
[198] P. W. Voorhees, *J. Stat. Phys.* **1985**, *38*, 231.
[199] H. Qiu, G. Chen, L. Sun, S. Hao, G. Han, C. Yang, *J. Mater. Chem.* **2011**, *21*, 17202.
[200] G. Chen, T. Y. Ohulchanskyy, S. Liu, W.-C. Law, F. Wu, M. T. Swihart, H. Ågren, P. N. Prasad, *ACS Nano* **2012**, *6*, 2969.
[201] Z. Gu, L. Yan, G. Tian, S. Li, Z. Chai, Y. Zhao, *Adv. Mater.* **2013**, *25*, 3758.
[202] L. Cheng, K. Yang, Y. Li, J. Chen, C. Wang, M. Shao, S.-T. Lee, Z. Liu, *Angew. Chem.* **2011**, *123*, 7523.
[203] B. Liu, Y. Chen, C. Li, F. He, Z. Hou, S. Huang, H. Zhu, X. Chen, J. Lin, *Adv. Funct. Mater.* **2015**, *25*, 4717.
[204] H. Xu, L. Cheng, C. Wang, X. Ma, Y. Li, Z. Liu, *Biomaterials* **2011**, *32*, 9364.
[205] G. Chen, J. Shen, T. Y. Ohulchanskyy, N. J. Patel, A. Kutikov, Z. Li, J. Song, R. K. Pandey, H. Ågren, P. N. Prasad, G. Han, *ACS Nano* **2012**, *6*, 8280.
[206] J. Jin, Y.-J. Gu, C. W.-Y. Man, J. Cheng, Z. Xu, Y. Zhang, H. Wang, V. H.-Y. Lee, S. H. Cheng, W.-T. Wong, *ACS Nano* **2011**, *5*, 7838.
[207] Y. Yang, Q. Shao, R. Deng, C. Wang, X. Teng, K. Cheng, Z. Cheng, L. Huang, Z. Liu, X. Liu, B. Xing, *Angew. Chem., Int. Ed.* **2012**, *51*, 3125.
[208] C. Liu, Z. Gao, J. Zeng, Y. Hou, F. Fang, Y. Li, R. Qiao, L. Shen, H. Lei, W. Yang, M. Gao, *ACS Nano* **2013**, *7*, 7227.
[209] W. Fan, B. Shen, W. Bu, F. Chen, K. Zhao, S. Zhang, L. Zhou, W. Peng, Q. Xiao, H. Xing, J. Liu, D. Ni, Q. He, J. Shi, *J. Am. Chem. Soc.* **2013**, *135*, 6494.
[210] L.-L. Li, R. Zhang, L. Yin, K. Zheng, W. Qin, P. R. Selvin, Y. Lu, *Angew. Chem.* **2012**, *124*, 6225.
[211] G. Tian, Z. Gu, L. Zhou, W. Yin, X. Liu, L. Yan, S. Jin, W. Ren, G. Xing, S. Li, Y. Zhao, *Adv. Mater.* **2012**, *24*, 1226.
[212] K. Liu, X. Liu, Q. Zeng, Y. Zhang, L. Tu, T. Liu, X. Kong, Y. Wang, F. Cao, S. A. G. Lambrechts, M. C. G. Aalders, H. Zhang, *ACS Nano* **2012**, *6*, 4054.
[213] Y. Li, J. Tang, D.-X. Pan, L.-D. Sun, C. Chen, Y. Liu, Y.-F. Wang, S. Shi, C.-H. Yan, *ACS Nano* **2016**, *10*, 2766.
[214] R. Deng, X. Xie, M. Vendrell, Y.-T. Chang, X. Liu, *J. Am. Chem. Soc.* **2011**, *133*, 20168.
[215] Y. Sun, X. Zhu, J. Peng, F. Li, *ACS Nano* **2013**, *7*, 11290.
[216] S. Zeng, Z. Yi, W. Lu, C. Qian, H. Wang, L. Rao, T. Zeng, H. Liu, H. Liu, B. Fei, J. Hao, *Adv. Funct. Mater.* **2014**, *24*, 4051.

[217] Q. Zhan, J. Qian, H. Liang, G. Somesfalean, D. Wang, S. He, Z. Zhang, S. Andersson-Engels, *ACS Nano* **2011**, *5*, 3744.
[218] M. Sun, L. Xu, W. Ma, X. Wu, H. Kuang, L. Wang, C. Xu, *Adv. Mater.* **2016**, *28*, 898.
[219] N. Wu, L. Bao, L. Ding, H. Ju, *Angew. Chem.* **2016**, *128*, 5306.
[220] M. He, P. Huang, C. Zhang, H. Hu, C. Bao, G. Gao, R. He, D. Cui, *Adv. Funct. Mater.* **2011**, *21*, 4470.
[221] J. Liu, Y. Liu, W. Bu, J. Bu, Y. Sun, J. Du, J. Shi, *J. Am. Chem. Soc.* **2014**, *136*, 9701.
[222] Q. Liu, M. Chen, Y. Sun, G. Chen, T. Yang, Y. Gao, X. Zhang, F. Li, *Biomaterials* **2011**, *32*, 8243.
[223] S. K. Maji, S. Sreejith, J. Joseph, M. Lin, T. He, Y. Tong, H. Sun, S. W.-K. Yu, Y. Zhao, *Adv. Mater.* **2014**, *26*, 5633.
[224] B. Dong, B. Cao, Y. He, Z. Liu, Z. Li, Z. Feng, *Adv. Mater.* **2012**, *24*, 1987.
[225] F. Chen, W. Bu, S. Zhang, X. Liu, J. Liu, H. Xing, Q. Xiao, L. Zhou, W. Peng, L. Wang, J. Shi, *Adv. Funct. Mater.* **2011**, *21*, 4285.
[226] L. Zeng, Y. Pan, R. Zou, J. Zhang, Y. Tian, Z. Teng, S. Wang, W. Ren, X. Xiao, J. Zhang, L. Zhang, A. Li, G. Lu, A. Wu, *Biomaterials* **2016**, *103*, 116.
[227] X. Ai, C. J. H. Ho, J. Aw, A. B. E. Attia, J. Mu, Y. Wang, X. Wang, Y. Wang, X. Liu, H. Chen, *Nat. Commun.* **2016**, *7*.
[228] F. He, G. Yang, P. Yang, Y. Yu, R. Lv, C. Li, Y. Dai, S. Gai, J. Lin, *Adv. Funct. Mater.* **2015**, *25*, 3966.
[229] Y. Chen, B. Liu, X. Deng, S. Huang, Z. Hou, C. Li, J. Lin, *Nanoscale* **2015**, *7*, 8574.
[230] Y. I. Park, K. T. Lee, Y. D. Suh, T. Hyeon, *Chem. Soc. Rev.* **2015**, *44*, 1302.
[231] W. Fan, W. Bu, J. Shi, *Adv. Mater.* **2016**, *28*, 3987.
[232] C. Wang, L. Cheng, Y. Liu, X. Wang, X. Ma, Z. Deng, Y. Li, Z. Liu, *Adv. Funct. Mater.* **2013**, *23*, 3077.
[233] Y. Dai, H. Xiao, J. Liu, Q. Yuan, P. a. Ma, D. Yang, C. Li, Z. Cheng, Z. Hou, P. Yang, J. Lin, *J. Am. Chem. Soc.* **2013**, *135*, 18920.
[234] Y. Min, J. Li, F. Liu, E. K. L. Yeow, B. Xing, *Angew. Chem., Int. Ed.* **2014**, *53*, 1012.
[235] S. S. Lucky, N. Muhammad Idris, Z. Li, K. Huang, K. C. Soo, Y. Zhang, *ACS Nano* **2015**, *9*, 191.
[236] Z. Hou, Y. Zhang, K. Deng, Y. Chen, X. Li, X. Deng, Z. Cheng, H. Lian, C. Li, J. Lin, *ACS Nano* **2015**, *9*, 2584.
[237] L. Zeng, Y. Pan, Y. Tian, X. Wang, W. Ren, S. Wang, G. Lu, A. Wu, *Biomaterials* **2015**, *57*, 93.
[238] L. e. Zhang, L. Zeng, Y. Pan, S. Luo, W. Ren, A. Gong, X. Ma, H. Liang, G. Lu, A. Wu, *Biomaterials* **2015**, *44*, 82.
[239] G. Yang, D. Yang, P. Yang, R. Lv, C. Li, C. Zhong, F. He, S. Gai, J. Lin, *Chem. Mater.* **2015**, *27*, 7957.
[240] Z. Hou, K. Deng, C. Li, X. Deng, H. Lian, Z. Cheng, D. Jin, J. Lin, *Biomaterials* **2016**, *101*, 32.
[241] Y.-H. Chien, Y.-L. Chou, S.-W. Wang, S.-T. Hung, M.-C. Liau, Y.-J. Chao, C.-H. Su, C.-S. Yeh, *ACS Nano* **2013**, *7*, 8516.
[242] C. Yue, C. Zhang, G. Alfranca, Y. Yang, X. Jiang, Y. Yang, F. Pan, J. M. de la Fuente, D. Cui, *Theranostics* **2016**, *6*, 456.
[243] B. Liu, C. Li, B. Xing, P. Yang, J. Lin, *J. Mater. Chem. B* **2016**, *4*, 4884.
[244] Z. Li, J. C. Barnes, A. Bosoy, J. F. Stoddart, J. I. Zink, *Chem. Soc. Rev.* **2012**, *41*, 2590.
[245] Q. He, J. Shi, *J. Mater. Chem.* **2011**, *21*, 5845.
[246] X. Huang, L. Li, T. Liu, N. Hao, H. Liu, D. Chen, F. Tang, *ACS Nano* **2011**, *5*, 5390.
[247] Q. He, Z. Zhang, F. Gao, Y. Li, J. Shi, *Small* **2011**, *7*, 271.
[248] Y. Zhao, X. Sun, G. Zhang, B. G. Trewyn, I. I. Slowing, V. S. Y. Lin, *ACS Nano* **2011**, *5*, 1366.
[249] H. Meng, M. Xue, T. Xia, Z. Ji, D. Y. Tarn, J. I. Zink, A. E. Nel, *ACS Nano* **2011**, *5*, 4131.
[250] H. Meng, S. Yang, Z. Li, T. Xia, J. Chen, Z. Ji, H. Zhang, X. Wang, S. Lin, C. Huang, Z. H. Zhou, J. I. Zink, A. E. Nel, *ACS Nano* **2011**, *5*, 4434.
[251] L. Pan, Q. He, J. Liu, Y. Chen, M. Ma, L. Zhang, J. Shi, *J. Am. Chem. Soc.* **2012**, *134*, 5722.
[252] M.-H. Kim, H.-K. Na, Y.-K. Kim, S.-R. Ryoo, H. S. Cho, K. E. Lee, H. Jeon, R. Ryoo, D.-H. Min, *ACS Nano* **2011**, *5*, 3568.
[253] S. Sreejith, X. Ma, Y. Zhao, *J. Am. Chem. Soc.* **2012**, *134*, 17346.
[254] C.-L. Zhu, C.-H. Lu, X.-Y. Song, H.-H. Yang, X.-R. Wang, *J. Am. Chem. Soc.* **2011**, *133*, 1278.
[255] N. Singh, A. Karambelkar, L. Gu, K. Lin, J. S. Miller, C. S. Chen, M. J. Sailor, S. N. Bhatia, *J. Am. Chem. Soc.* **2011**, *133*, 19582.
[256] Q. He, Y. Gao, L. Zhang, Z. Zhang, F. Gao, X. Ji, Y. Li, J. Shi, *Biomaterials* **2011**, *32*, 7711.
[257] H. Yan, C. Teh, S. Sreejith, L. Zhu, A. Kwok, W. Fang, X. Ma, K. T. Nguyen, V. Korzh, Y. Zhao, *Angew. Chem. Int. Ed.* **2012**, *51*, 8373.
[258] Y. Gao, Y. Chen, X. Ji, X. He, Q. Yin, Z. Zhang, J. Shi, Y. Li, *ACS Nano* **2011**, *5*, 9788.
[259] Y. Chen, K. Ai, J. Liu, G. Sun, Q. Yin, L. Lu, *Biomaterials* **2015**, *60*, 111.
[260] Q. Zhang, F. Liu, K. T. Nguyen, X. Ma, X. Wang, B. Xing, Y. Zhao, *Adv. Funct. Mater.* **2012**, *22*, 5144.
[261] Q. Zhang, X. Wang, P.-Z. Li, K. T. Nguyen, X.-J. Wang, Z. Luo, H. Zhang, N. S. Tan, Y. Zhao, *Adv. Funct. Mater.* **2014**, *24*, 2450.
[262] H. P. Rim, K. H. Min, H. J. Lee, S. Y. Jeong, S. C. Lee, *Angew. Chem. Int. Ed.* **2011**, *50*, 8853.
[263] F. Muhammad, M. Guo, W. Qi, F. Sun, A. Wang, Y. Guo, G. Zhu, *J. Am. Chem. Soc.* **2011**, *133*, 8778.
[264] Z. Luo, K. Cai, Y. Hu, L. Zhao, P. Liu, L. Duan, W. Yang, *Angew. Chem. Int. Ed.* **2011**, *50*, 640.
[265] Z. Zhao, H. Meng, N. Wang, M. J. Donovan, T. Fu, M. You, Z. Chen, X. Zhang, W. Tan, *Angew. Chem., Int. Ed.* **2013**, *52*, 7487.
[266] S. H. van Rijt, D. A. Bölükbas, C. Argyo, S. Datz, M. Lindner, O. Eickelberg, M. Königshoff, T. Bein, S. Meiners, *ACS Nano* **2015**, *9*, 2377.
[267] C. E. Ashley, E. C. Carnes, K. E. Epler, D. P. Padilla, G. K. Phillips, R. E. Castillo, D. C. Wilkinson, B. S. Wilkinson, C. A. Burgard, R. M. Kalinich, J. L. Townson, B. Chackerian, C. L. Willman, D. S. Peabody, W. Wharton, C. J. Brinker, *ACS Nano* **2012**, *6*, 2174.
[268] S. A. Mackowiak, A. Schmidt, V. Weiss, C. Argyo, C. von Schirnding, T. Bein, C. Bräuchle, *Nano Lett.* **2013**, *13*, 2576.
[269] X. Liu, A. Situ, Y. Kang, K. R. Villabroza, Y. Liao, C. H. Chang, T. Donahue, A. E. Nel, H. Meng, *ACS Nano* **2016**, *10*, 2702.
[270] Z. Zhang, D. Balogh, F. Wang, I. Willner, *J. Am. Chem. Soc.* **2013**, *135*, 1934.
[271] Y.-L. Zhao, J. F. Stoddart, *Acc. Chem. Res.* **2009**, *42*, 1161.
[272] G. Hong, S. Diao, A. L. Antaris, H. Dai, *Chem. Rev.* **2015**, *115*, 10816.
[273] M. I. Sajid, U. Jamshaid, T. Jamshaid, N. Zafar, H. Fessi, A. Elaissari, *Int. J. Pharm.* **2016**, *501*, 278.
[274] M. Lamberti, P. Pedata, N. Sannolo, S. Porto, A. De Rosa, M. Caraglia, *Int. J. Immunopathol. Pharmacol.* **2015**, *28*, 4.
[275] Y. Zhang, D. Petibone, Y. Xu, M. Mahmood, A. Karmakar, D. Casciano, S. Ali, A. S. Biris, *Drug Metab. Rev.* **2014**, *46*, 232.
[276] F. A. Murphy, C. A. Poland, R. Duffin, K. T. Al-Jamal, H. Ali-Boucetta, A. Nunes, F. Byrne, A. Prina-Mello, Y. Volkov, S. Li, S. J. Mather, A. Bianco, M. Prato, W. MacNee, W. A. Wallace, K. Kostarelos, K. Donaldson, *Am. J. Pathol.* **2011**, *178*, 2587.
[277] S. Sachar, R. K. Saxena, *PLoS One* **2011**, *6*, e22032.
[278] G. Bardi, A. Nunes, L. Gherardini, K. Bates, K. T. Al-Jamal, C. Gaillard, M. Prato, A. Bianco, T. Pizzorusso, K. Kostarelos, *PLoS One* **2013**, *8*, e80964.
[279] D. Roxbury, J. Mittal, A. Jagota, *Nano Lett.* **2012**, *12*, 1464.
[280] S. Diao, G. Hong, J. T. Robinson, L. Jiao, A. L. Antaris, J. Z. Wu, C. L. Choi, H. Dai, *J. Am. Chem. Soc.* **2012**, *134*, 16971.
[281] J. Yang, Q. Zhao, M. Lyu, Z. Zhang, X. Wang, M. Wang, Z. Gao, Y. Li, *Small* **2016**, *12*, 3164.

[282] J. P. Giraldo, M. P. Landry, S.-Y. Kwak, R. M. Jain, M. H. Wong, N. M. Iverson, M. Ben-Naim, M. S. Strano, *Small* **2015**, *11*, 3973.
[283] A. L. Antaris, J. T. Robinson, O. K. Yaghi, G. Hong, S. Diao, R. Luong, H. Dai, *ACS Nano* **2013**, *7*, 3644.
[284] N. Gao, Q. Zhang, Q. Mu, Y. Bai, L. Li, H. Zhou, E. R. Butch, T. B. Powell, S. E. Snyder, G. Jiang, B. Yan, *ACS Nano* **2011**, *5*, 4581.
[285] J. Liu, C. Wang, X. Wang, X. Wang, L. Cheng, Y. Li, Z. Liu, *Adv. Funct. Mater.* **2015**, *25*, 384.
[286] T.-G. Cha, B. A. Baker, M. D. Sauffer, J. Salgado, D. Jaroch, J. L. Rickus, D. M. Porterfield, J. H. Choi, *ACS Nano* **2011**, *5*, 4236.
[287] P. D. Boyer, S. Ganesh, Z. Qin, B. D. Holt, M. J. Buehler, M. F. Islam, K. N. Dahl, *ACS Appl. Mater. Interfaces* **2016**, *8*, 3524.
[288] P. Kesharwani, V. Mishra, N. K. Jain, *Drug Discovery Today* **2015**, *20*, 1049.
[289] A. Elhissi, W. Ahmed, I. U. Hassan, V. R. Dhanak, A. D'Emanuele, *J. Drug Delivery* **2011**, 2012.
[290] S. Diao, J. L. Blackburn, G. Hong, A. L. Antaris, J. Chang, J. Z. Wu, B. Zhang, K. Cheng, C. J. Kuo, H. Dai, *Angew. Chem.* **2015**, *127*, 14971.
[291] K. Welsher, S. P. Sherlock, H. Dai, *Proc. Natl. Acad. Sci. USA* **2011**, *108*, 8943.
[292] J. T. Robinson, G. Hong, Y. Liang, B. Zhang, O. K. Yaghi, H. Dai, *J. Am. Chem. Soc.* **2012**, *134*, 10664.
[293] H. Yi, D. Ghosh, M.-H. Ham, J. Qi, P. W. Barone, M. S. Strano, A. M. Belcher, *Nano Lett.* **2012**, *12*, 1176.
[294] G. Hong, S. M. Tabakman, K. Welsher, Z. Chen, J. T. Robinson, H. Wang, B. Zhang, H. Dai, *Angew. Chem., Int. Ed.* **2011**, *50*, 4644.
[295] G. Hong, J. C. Lee, J. T. Robinson, U. Raaz, L. Xie, N. F. Huang, J. P. Cooke, H. Dai, *Nat. Med.* **2012**, *18*, 1841.
[296] G. Hong, S. Diao, J. Chang, A. L. Antaris, C. Chen, B. Zhang, S. Zhao, D. N. Atochin, P. L. Huang, K. I. Andreasson, C. J. Kuo, H. Dai, *Nat. Photon.* **2014**, *8*, 723.
[297] N. M. Iverson, P. W. Barone, M. Shandell, L. J. Trudel, S. Sen, F. Sen, V. Ivanov, E. Atolia, E. Farias, T. P. McNicholas, N. Reuel, N. M. A. Parry, G. N. Wogan, M. S. Strano, *Nat. Nanotechnol.* **2013**, *8*, 873.
[298] N. M. Bardhan, D. Ghosh, A. M. Belcher, *Nat. Commun.* **2014**, *5*, 4918.
[299] A. E. Goode, D. A. Gonzalez Carter, M. Motskin, I. S. Pienaar, S. Chen, S. Hu, P. Ruenraroengsak, M. P. Ryan, M. S. P. Shaffer, D. T. Dexter, A. E. Porter, *Biomaterials* **2015**, *70*, 57.
[300] P. Ruenraroengsak, S. Chen, S. Hu, J. Melbourne, S. Sweeney, A. J. Thorley, J. N. Skepper, M. S. P. Shaffer, T. D. Tetley, A. E. Porter, *ACS Nano* **2016**, *10*, 5070.
[301] N. Fakhri, A. D. Wessel, C. Willms, M. Pasquali, D. R. Klopfenstein, F. C. MacKintosh, C. F. Schmidt, *Science* **2014**, *344*, 1031.
[302] S. Prakash, M. Malhotra, W. Shao, C. Tomaro-Duchesneau, S. Abbasi, *Adv. Drug Delivery Rev.* **2011**, *63*, 1340.
[303] H. Wu, G. Liu, X. Wang, J. Zhang, Y. Chen, J. Shi, H. Yang, H. Hu, S. Yang, *Acta Biomater.* **2011**, *7*, 3496.
[304] M. Zhou, S. Liu, Y. Jiang, H. Ma, M. Shi, Q. Wang, W. Zhong, W. Liao, M. M. Q. Xing, *Adv. Funct. Mater.* **2015**, *25*, 4730.
[305] Z. Ji, G. Lin, Q. Lu, L. Meng, X. Shen, L. Dong, C. Fu, X. Zhang, *J. Colloid Interface Sci.* **2012**, *365*, 143.
[306] L. Meng, X. Zhang, Q. Lu, Z. Fei, P. J. Dyson, *Biomaterials* **2012**, *33*, 1689.
[307] M. Das, S. R. Datir, R. P. Singh, S. Jain, *Mol. Pharm.* **2013**, *10*, 2543.
[308] A. Razzazan, F. Atyabi, B. Kazemi, R. Dinarvand, *Mater. Sci. Eng., C* **2016**, *62*, 614.
[309] C. Guo, W. T. Al-Jamal, F. M. Toma, A. Bianco, M. Prato, K. T. Al-Jamal, K. Kostarelos, *Bioconjugate Chem.* **2015**, *26*, 1370.
[310] H. Li, X. Fan, X. Chen, *ACS Appl. Mater. Interfaces* **2016**, *8*, 4500.
[311] E. Heister, V. Neves, C. Lamprecht, S. R. P. Silva, H. M. Coley, J. McFadden, *Carbon* **2012**, *50*, 622.
[312] P.-C. Lee, C.-L. Peng, M.-J. Shieh, *J. Controlled Release* **2016**, *225*, 140.
[313] H. Wu, G. Liu, Y. Zhuang, D. Wu, H. Zhang, H. Yang, H. Hu, S. Yang, *Biomaterials* **2011**, *32*, 4867.
[314] M.-L. Chen, Y.-J. He, X.-W. Chen, J.-H. Wang, *Langmuir* **2012**, *28*, 16469.
[315] X. Liu, I. Marangon, G. Melinte, C. Wilhelm, C. Ménard-Moyon, B. P. Pichon, O. Ersen, K. Aubertin, W. Baaziz, C. Pham-Huu, S. Bégin-Colin, A. Bianco, F. Gazeau, D. Bégin, *ACS Nano* **2014**, *8*, 11290.
[316] B. Czarny, D. Georgin, F. Berthon, G. Plastow, M. Pinault, G. Patriarche, A. Thuleau, M. M. L'Hermite, F. Taran, V. Dive, *ACS Nano* **2014**, *8*, 5715.
[317] J. Ren, S. Shen, D. Wang, Z. Xi, L. Guo, Z. Pang, Y. Qian, X. Sun, X. Jiang, *Biomaterials* **2012**, *33*, 3324.
[318] X. Liu, H. Tao, K. Yang, S. Zhang, S.-T. Lee, Z. Liu, *Biomaterials* **2011**, *32*, 144.
[319] R. Singh, S. V. Torti, *Adv. Drug Delivery Rev.* **2013**, *65*, 2045.
[320] C. Liang, S. Diao, C. Wang, H. Gong, T. Liu, G. Hong, X. Shi, H. Dai, Z. Liu, *Adv. Mater.* **2014**, *26*, 5646.
[321] F. Zhou, S. Wu, B. Wu, W. R. Chen, D. Xing, *Small* **2011**, *7*, 2727.
[322] F. Zhou, S. Wu, S. Song, W. R. Chen, D. E. Resasco, D. Xing, *Biomaterials* **2012**, *33*, 3235.
[323] L. García-Hevia, J. C. Villegas, F. Fernández, Í. Casafont, J. González, R. Valiente, M. L. Fanarraga, *Adv. Healthcare Mater.* **2016**, *5*, 1080.
[324] X. Wang, C. Wang, L. Cheng, S.-T. Lee, Z. Liu, *J. Am. Chem. Soc.* **2012**, *134*, 7414.
[325] L. Wang, J. Shi, H. Zhang, H. Li, Y. Gao, Z. Wang, H. Wang, L. Li, C. Zhang, C. Chen, Z. Zhang, Y. Zhang, *Biomaterials* **2013**, *34*, 262.
[326] T. Sada, T. Fujigaya, Y. Niidome, K. Nakazawa, N. Nakashima, *ACS Nano* **2011**, *5*, 4414.
[327] M. Nasrollahzadeh, F. Babaei, P. Fakhri, B. Jaleh, *RSC Adv.* **2015**, *5*, 10782.
[328] L. Yan, Y. Wang, X. Xu, C. Zeng, J. Hou, M. Lin, J. Xu, F. Sun, X. Huang, L. Dai, F. Lu, Y. Liu, *Chem. Res. Toxicol.* **2012**, *25*, 1265.
[329] K. Yang, H. Gong, X. Shi, J. Wan, Y. Zhang, Z. Liu, *Biomaterials* **2013**, *34*, 2787.
[330] D. Zhang, Z. Zhang, Y. Liu, M. Chu, C. Yang, W. Li, Y. Shao, Y. Yue, R. Xu, *Biomaterials* **2015**, *68*, 100.
[331] K. Wang, J. Ruan, H. Song, J. Zhang, Y. Wo, S. Guo, D. Cui, *Nanoscale Res. Lett.* **2011**, *6*, 1.
[332] H. Ali-Boucetta, D. Bitounis, R. Raveendran-Nair, A. Servant, J. Van den Bossche, K. Kostarelos, *Adv. Healthcare Mater.* **2013**, *2*, 433.
[333] S. A. Sydlik, S. Jhunjhunwala, M. J. Webber, D. G. Anderson, R. Langer, *ACS Nano* **2015**, *9*, 3866.
[334] Y. Liu, Y. Luo, J. Wu, Y. Wang, X. Yang, R. Yang, B. Wang, J. Yang, N. Zhang, *Sci. Rep.* **2013**, *3*, 3469.
[335] G. Qu, X. Wang, Q. Liu, R. Liu, N. Yin, J. Ma, L. Chen, J. He, S. Liu, G. Jiang, *J. Environ. Sci.* **2013**, *25*, 873.
[336] S. Mukherjee, P. Sriram, A. K. Barui, S. K. Nethi, V. Veeriah, S. Chatterjee, K. I. Suresh, C. R. Patra, *Adv. Healthcare Mater.* **2015**, *4*, 1722.
[337] J. Qian, D. Wang, F.-H. Cai, W. Xi, L. Peng, Z.-F. Zhu, H. He, M.-L. Hu, S. He, *Angew. Chem. Int. Ed.* **2012**, *51*, 10570.
[338] H. Hong, Y. Zhang, J. W. Engle, T. R. Nayak, C. P. Theuer, R. J. Nickles, T. E. Barnhart, W. Cai, *Biomaterials* **2012**, *33*, 4147.
[339] H. Hong, K. Yang, Y. Zhang, J. W. Engle, L. Feng, Y. Yang, T. R. Nayak, S. Goel, J. Bean, C. P. Theuer, T. E. Barnhart, Z. Liu, W. Cai, *ACS Nano* **2012**, *6*, 2361.
[340] H. Qin, T. Zhou, S. Yang, D. Xing, *Small* **2015**, *11*, 2675.

[341] H. Moon, D. Kumar, H. Kim, C. Sim, J.-H. Chang, J.-M. Kim, H. Kim, D.-K. Lim, *ACS Nano* **2015**, *9*, 2711.
[342] Z. Sheng, L. Song, J. Zheng, D. Hu, M. He, M. Zheng, G. Gao, P. Gong, P. Zhang, Y. Ma, L. Cai, *Biomaterials* **2013**, *34*, 5236.
[343] G.-Y. Chen, C.-L. Chen, H.-Y. Tuan, P.-X. Yuan, K.-C. Li, H.-J. Yang, Y.-C. Hu, *Adv. Healthcare Mater.* **2014**, *3*, 1486.
[344] W. Wang, N. Han, R. Li, W. Han, X. Zhang, F. Li, *Anal. Chem.* **2015**, *87*, 9302.
[345] X. Wang, Q. Li, J. Xu, S. Wu, T. Xiao, J. Hao, P. Yu, L. Mao, *Anal. Chem.* **2016**.
[346] K. Yang, J. Wan, S. Zhang, B. Tian, Y. Zhang, Z. Liu, *Biomaterials* **2012**, *33*, 2206.
[347] B. Tian, C. Wang, S. Zhang, L. Feng, Z. Liu, *ACS Nano* **2011**, *5*, 7000.
[348] W. Zhang, Z. Guo, D. Huang, Z. Liu, X. Guo, H. Zhong, *Biomaterials* **2011**, *32*, 8555.
[349] O. Akhavan, E. Ghaderi, *Small* **2013**, *9*, 3593.
[350] J. T. Robinson, S. M. Tabakman, Y. Liang, H. Wang, H. Sanchez Casalongue, D. Vinh, H. Dai, *J. Am. Chem. Soc.* **2011**, *133*, 6825.
[351] S. M. Sharker, J. E. Lee, S. H. Kim, J. H. Jeong, I. In, H. Lee, S. Y. Park, *Biomaterials* **2015**, *61*, 229.
[352] U. Dembereldorj, M. Kim, S. Kim, E.-O. Ganbold, S. Y. Lee, S.-W. Joo, *J. Mater. Chem.* **2012**, *22*, 23845.
[353] P. Kalluru, R. Vankayala, C.-S. Chiang, K. C. Hwang, *Biomaterials* **2016**, *95*, 1.
[354] L. Zhang, Z. Lu, Q. Zhao, J. Huang, H. Shen, Z. Zhang, *Small* **2011**, *7*, 460.
[355] G. Ni, Y. Wang, X. Wu, X. Wang, S. Chen, X. Liu, *Immunol. Lett.* **2012**, *148*, 126.
[356] G. Gollavelli, Y.-C. Ling, *Biomaterials* **2012**, *33*, 2532.
[357] A.-A. Nahain, J.-E. Lee, J. H. Jeong, S. Y. Park, *Biomacromolecules* **2013**, *14*, 4082.
[358] M. Yi, S. Yang, Z. Peng, C. Liu, J. Li, W. Zhong, R. Yang, W. Tan, *Anal. Chem.* **2014**, *86*, 3548.
[359] C. Meng, X. Zhi, C. Li, C. Li, Z. Chen, X. Qiu, C. Ding, L. Ma, H. Lu, D. Chen, G. Liu, D. Cui, *ACS Nano* **2016**, *10*, 2203.
[360] B. Cornelissen, S. Able, V. Kersemans, P. A. Waghorn, S. Myhra, K. Jurkshat, A. Crossley, K. A. Vallis, *Biomaterials* **2013**, *34*, 1146.
[361] W. Miao, G. Shim, S. Lee, S. Lee, Y. S. Choe, Y.-K. Oh, *Biomaterials* **2013**, *34*, 3402.
[362] S. H. Kim, J. E. Lee, S. M. Sharker, J. H. Jeong, I. In, S. Y. Park, *Biomacromolecules* **2015**, *16*, 3519.
[363] P. Huang, C. Xu, J. Lin, C. Wang, X. Wang, C. Zhang, X. Zhou, S. Guo, D. Cui, *Theranostics* **2011**, *1*, 240.
[364] Y. Zhang, J. F. Lovell, *Theranostics* **2012**, *2*, 905.
[365] H. Huang, W. Song, J. Rieffel, J. F. Lovell, *Front. Phys.* **2015**, 3.
[366] Y. Zhang, J. F. Lovell, *WIRES: Nanomed. Nanobiotechnol.* **2016**, DOI: 10.1002/wnan.1420.
[367] P. P. Ghoroghchian, P. R. Frail, K. Susumu, D. Blessington, A. K. Brannan, F. S. Bates, B. Chance, D. A. Hammer, M. J. Therien, *Proc. Natl. Acad. Sci. USA* **2005**, *102*, 2922.
[368] J. F. Lovell, C. S. Jin, E. Huynh, T. D. MacDonald, W. Cao, G. Zheng, *Angew. Chem., Int. Ed.* **2012**, *51*, 2429.
[369] E. Huynh, G. Zheng, *Nano Today* **2014**, *9*, 212.
[370] C.-Y. Hsu, M.-P. Nieh, P.-S. Lai, *Chem. Commun.* **2012**, *48*, 9343.
[371] J.-H. Lee, S. Shao, K. T. Cheng, J. F. Lovell, C. H. Paik, *J. Liposome Res.* **2015**, *25*, 101.
[372] C. S. Jin, J. F. Lovell, J. Chen, G. Zheng, *ACS Nano* **2013**, *7*, 2541.
[373] W. Viricel, A. Mbarek, J. Leblond, *Angew. Chem.* **2015**, *127*, 12934.
[374] A. K. Rengan, A. B. Bukhari, A. Pradhan, R. Malhotra, R. Banerjee, R. Srivastava, A. De, *Nano Lett.* **2015**, *15*, 842.
[375] X.-D. Xu, L. Zhao, Q. Qu, J.-G. Wang, H. Shi, Y. Zhao, *ACS Appl. Mater. Interfaces* **2015**, *7*, 17371.
[376] A. K. Rengan, M. Jagtap, A. De, R. Banerjee, R. Srivastava, *Nanoscale* **2014**, *6*, 916.
[377] V. Saxena, C. Gacchina Johnson, A. H. Negussie, K. V. Sharma, M. R. Dreher, B. J. Wood, *Int. J. Hyperthermia* **2015**, *31*, 67.
[378] C. S. Jin, L. Cui, F. Wang, J. Chen, G. Zheng, *Adv. Healthcare Mater.* **2014**, *3*, 1240.
[379] K. A. Carter, S. Shao, M. I. Hoopes, D. Luo, B. Ahsan, V. M. Grigoryants, W. Song, H. Huang, G. Zhang, R. K. Pandey, J. Geng, B. A. Pfeifer, C. P. Scholes, J. Ortega, M. Karttunen, J. F. Lovell, *Nat. Commun.* **2014**, 5.
[380] E. Huynh, J. F. Lovell, R. Fobel, G. Zheng, *Small* **2014**, *10*, 1184.
[381] D. Luo, K. A. Carter, A. Razi, J. Geng, S. Shao, C. Lin, J. Ortega, J. F. Lovell, *J. Controlled Release* **2015**, *220*, Part A, 484.
[382] D. Luo, N. Li, K. A. Carter, C. Lin, J. Geng, S. Shao, W.-C. Huang, Y. Qin, G. E. Atilla-Gokcumen, J. F. Lovell, *Small* **2016**, *12*, 3039.
[383] D. Luo, K. A. Carter, A. Razi, J. Geng, S. Shao, D. Giraldo, U. Sunar, J. Ortega, J. F. Lovell, *Biomaterials* **2016**, *75*, 193.
[384] K. A. Carter, S. Wang, J. Geng, D. Luo, S. Shao, J. F. Lovell, *Mol. Pharm.* **2016**, *13*, 420.
[385] C. S. Jin, J. F. Lovell, G. Zheng, *J. Vis. Exp.* **2013**, 50536.
[386] N. Muhanna, C. S. Jin, E. Huynh, H. Chan, Y. Qiu, W. Jiang, L. Cui, L. Burgess, M. K. Akens, J. Chen, J. C. Irish, G. Zheng, *Theranostics* **2015**, *5*, 1428.
[387] S. Shao, J. Geng, H. Ah Yi, S. Gogia, S. Neelamegham, A. Jacobs, J. F. Lovell, *Nat. Chem.* **2015**, *7*, 438.
[388] L. Cui, D. Tokarz, R. Cisek, K. K. Ng, F. Wang, J. Chen, V. Barzda, G. Zheng, *Angew. Chem. Int. Ed.* **2015**, *54*, 13928.
[389] K. K. Ng, M. Takada, C. C. S. Jin, G. Zheng, *Bioconjugate Chem.* **2015**, *26*, 345.
[390] N. C. M. Tam, P. Z. McVeigh, T. D. MacDonald, A. Farhadi, B. C. Wilson, G. Zheng, *Bioconjugate Chem.* **2012**, *23*, 1726.
[391] T. D. MacDonald, T. W. Liu, G. Zheng, *Angew. Chem., Int. Ed.* **2014**, *53*, 6956.
[392] C. S. Jin, M. Overchuk, L. Cui, B. C. Wilson, R. G. Bristow, J. Chen, G. Zheng, *Prostate* **2016**.
[393] T. W. Liu, T. D. MacDonald, J. Shi, B. C. Wilson, G. Zheng, *Angew. Chem. Int. Ed.* **2012**, *51*, 13128.
[394] T. W. Liu, T. D. MacDonald, C. S. Jin, J. M. Gold, R. G. Bristow, B. C. Wilson, G. Zheng, *ACS Nano* **2013**, *7*, 4221.
[395] N. C. Ni, C. S. Jin, L. Cui, Z. Shao, J. Wu, S.-H. Li, R. D. Weisel, G. Zheng, R.-K. Li, *Mol. Imaging Biol.* **2016**, 1.